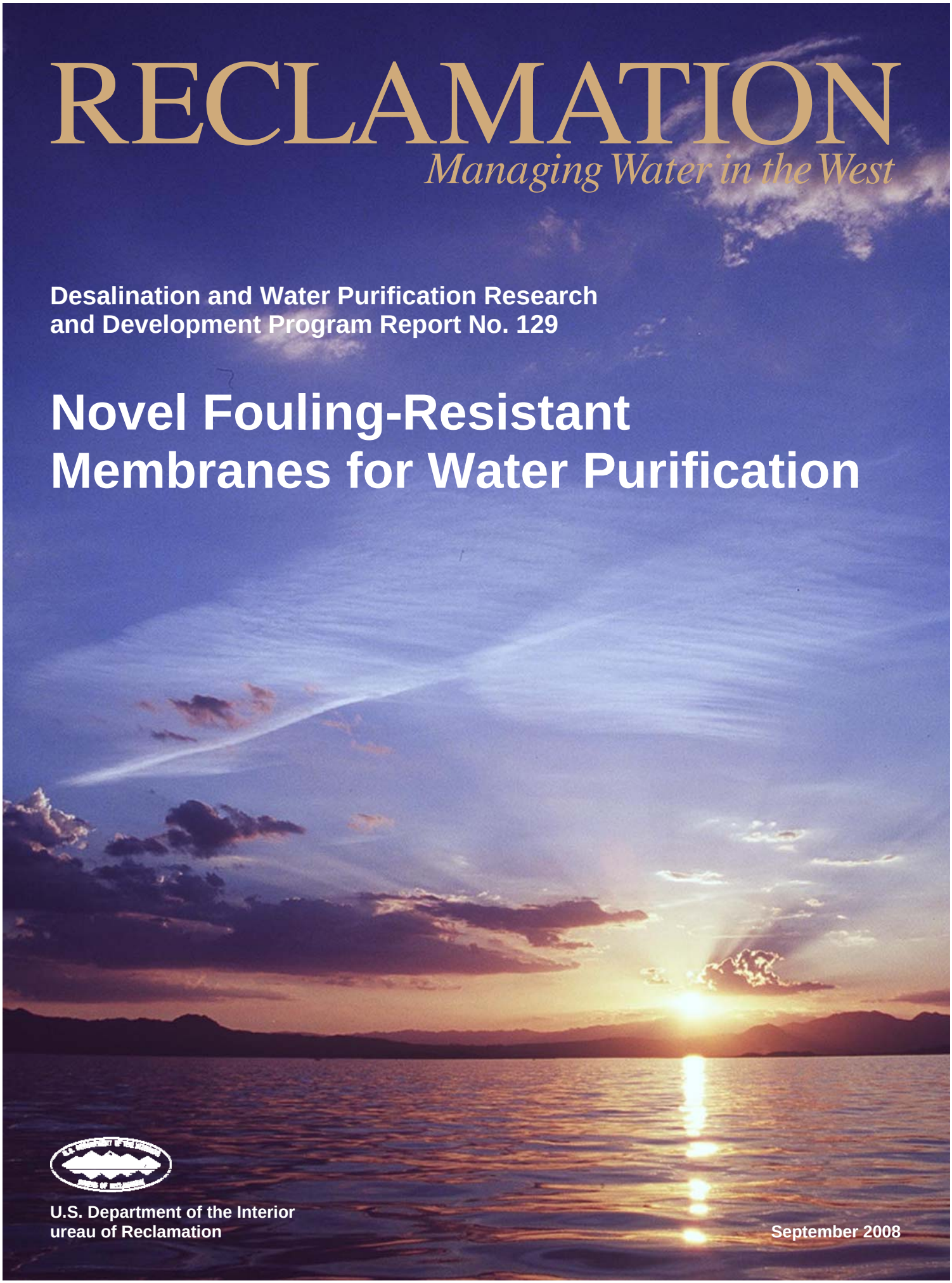

RECLAMATION

*Managing Water in the West*

**Desalination and Water Purification Research and Development Program Report No. 129**

# Novel Fouling-Resistant Membranes for Water Purification

**U.S. Department of the Interior**
**ureau of Reclamation**

**September 2008**

# REPORT DOCUMENTATION PAGE

*Form Approved*
*OMB No. 0704-0188*



| 1. REPORT DATE *(DD-MM-YYYY)* | 2. REPORT TYPE | 3. DATES COVERED *(From - To)* |
|---|---|---|
| March 2006 | Final | October 2004–September 2005 |

**4. TITLE AND SUBTITLE**
Novel Fouling-Resistant Membranes for Water Purification

**5a. CONTRACT NUMBER**
Agreement No. 04-FC-81-1042

**5b. GRANT NUMBER**

**5c. PROGRAM ELEMENT NUMBER**

**6. AUTHOR(S)**
Hao Ju and Benny D. Freeman

**5d. PROJECT NUMBER**

**5e. TASK NUMBER**
Task A

**5f. WORK UNIT NUMBER**

**7. PERFORMING ORGANIZATION NAME(S) AND ADDRESS(ES)**
The University of Texas at Austin
Department of Chemical Engineering
Center for Energy and Environmental Resources
10100 Burnet Road, Bldg. 133
Austin, TX 78758

**8. PERFORMING ORGANIZATION REPORT NUMBER**

**9. SPONSORING / MONITORING AGENCY NAME(S) AND ADDRESS(ES)**
U.S. Department of the Interior
Bureau of Reclamation,
Denver Federal Center
PO Box 25007, Denver CO 80225-0007

**10. SPONSOR/MONITOR'S ACRONYM(S)**
Reclamation

**11. SPONSOR/MONITOR'S REPORT NUMBER(S)**
DWPR Report No. 129

**12. DISTRIBUTION / AVAILABILITY STATEMENT**
Available from the National Technical Information Service
Operations Division, 5285 Port Royal Road, Springfield VA 22161

**13. SUPPLEMENTARY NOTES**
Report can be downloaded from Reclamation Web site:
www.usbr.gov/pmts/water/publications/reports.html

**14. ABSTRACT** ***(Maximum 200 words)***

Ultrafiltration (UF), nanofiltration (NF), and reverse osmosis (RO) processes have been widely used in water purification, especially for removal of organics and/or desalination. An approach of applying a very thin coating of fouling-resistant polymer to the membrane surface has been developed to increase the oil/water fouling resistance of commercially available UF, NF, and RO membranes. These coating polymers are crosslinked polyethylene glycol diacrylate networks, which exhibit high water permeability, excellent rejection of organic components in oil/water emulsions, and good fouling resistance. Commercial poly(vinylidene fluoride) (PVDF) and polysulfone (PSF) UF membranes were selected as support membranes. Scanning electron microscopy (SEM), x-ray photoelectron spectroscopy (XPS), and contact angle measurement were applied to examine the surface characteristics of coated PSF membranes. Dynamic oil fouling filtration experiments in dead-end and crossflow modes were performed using well-characterized oil/water emulsions, and the coated PSF membranes showed water flux values about five times higher than those of uncoated PSF membranes.

**15. SUBJECT TERMS**
desalination, ultrafiltration, produced water, membrane, fouling resistance, polysulfone

| 16. SECURITY CLASSIFICATION OF: | | | 17. LIMITATION OF ABSTRACT | 18. NUMBER OF PAGES | 19a. NAME OF RESPONSIBLE PERSON |
|---|---|---|---|---|---|
| a. REPORT | b. ABSTRACT | c. THIS PAGE | | | Saied Delagah |
| UL | UL | UL | SAR | 62 | 19b. TELEPHONE NUMBER *(include area code)* 303-445-2248 |

**Desalination and Water Purification Research and Development Program Report No. 129**

# Novel Fouling-Resistant Membranes for Water Purification

**Prepared for Reclamation Under Agreement No. 04-FC-81-1042**

*by*

**Hao Ju**
**Benny D. Freeman**
**University of Texas at Austin**
**Austin, Texas**

**U.S. Department of the Interior**
**Bureau of Reclamation**
**Technical Service Center**
**Water and Environmental Services Division**
**Water Treatment Engineering Research Team**
**Denver, Colorado**

**September 2008**

## MISSION STATEMENTS

The mission of the Department of the Interior is to protect and provide access to our Nation's natural and cultural heritage and honor our trust responsibilities to Indian tribes and our commitments to island communities.

---

The mission of the Bureau of Reclamation is to manage, develop, and protect water and related resources in an environmentally and economically sound manner in the interest of the American public.

## Disclaimer

The views, analysis, recommendations, and conclusions in this report are those of the authors and do not represent official or unofficial policies or opinions of the United States Government, and the United States takes no position with regard to any findings, conclusions, or recommendations made. As such, mention of trade names or commercial products does not constitute their endorsement by the United States Government.

# Acknowledgement

The Desalination and Water Purification Research and Development Program of the Bureau of Reclamation kindly provided funding for this project.

Our special thanks are due to the Water Treatment Engineering and Research Group at the Bureau of Reclamation for their help. We also thank the following individuals for their contribution to this project:

Saied Delagah, Katie Benko, and Michelle Chapman (Bureau of Reclamation)

Bryan McCloskey, Elizabeth Van Wanger, Alyson Sagle, Yuan-Hsuan Wu, Ho Bum Park, Leah Shimko, Jeff Nason, Desmond Lawler and Douglas Lloyd (University of Texas at Austin).

# Abbreviations and Acronyms

| | |
|---|---|
| μm | micrometer |
| atm | atmospheric pressure |
| CWA | Clean Water Act |
| $d_i$ | droplet diameter |
| $D_n$ | number average diameter |
| $D_v$ | volume or mass average diameter |
| DC193 | a copolymer of poly(dimethylsiloxane) and poly(ethylene oxide) from Dow Chemical, surfactant |
| EPA | Environment Protection Agency |
| FT-IR/ATR | Fourier transform infrared/attenuated total reflectance |
| $g/cm^3$ | gram per cubic centimeter |
| GE | General Electric |
| gpm | gallons per minute |
| HPK | 1-hydrooxycyclohexyl phenyl ketone, photoinitiator |
| JMP | software for experimental design |
| $L/(m^2\ hr)$ | liter per square meter per hour |
| $M_n$ | number average molecular weight of polymer |
| $N_i$ | number of droplets with a diameter of $d_i$ |
| NF | nanofiltration |
| nm | nanometer |
| PEG | poly(ethylene glycol) |
| PEGA | poly(ethylene glycol acrylate) |
| PEGDA | poly(ethylene glycol diacrylate) |
| PEGMEA | poly(ethylene glycol methyl ether acrylate) |
| PEO | poly(ethylene oxide) |
| PES | poly(ether sulfone) |
| ppm | parts per million |
| PSF | polysulfone |
| psi | pounds per square inch |
| PVDF | poly(vinylidene fluoride) |
| RO | reverse osmosis |
| rpm | revolutions per minute |
| SEM | scanning electron microscopy |

## Abbreviations and Acronyms (continued)

| | |
|---|---|
| TDS | total dissolved solids |
| TMI | Texas Materials Institute |
| TMP | transmembrane pressure |
| UF | ultrafiltration |
| UT | University of Texas at Austin |
| UV | ultraviolet |
| wt. % | weight percent |
| XPS | x-ray photoelectron spectroscopy |

# Table of Contents

# List of Figures

## List of Figures (continued)

## List of Figures (continued)

# List of Tables

# 1. Executive Summary

The objective of this experimental research program was to provide new alternatives to purify produced water by removal of emulsified oil, particulates, and dissolved solids in order to enable inexpensive beneficial use of produced water in applications such as agricultural and landscape irrigation and drinking water. Such beneficial use could significantly reduce injection costs associated with current disposal practices for produced water and provide, at least temporarily, a new source of purified water in what are often water-starved regions.

This objective has been achieved by exploiting recent discoveries that dramatically improve the fouling resistance of polymer membranes. We have developed new, fouling-reducing membrane coatings and applied them to commercially available poly(vinylidene fluoride) (PVDF) and polysulfone (PSF) ultrafiltration (UF) membranes to provide reductions in membrane fouling and marked improvements in membrane lifetime for produced water purification. These coating polymers are crosslinked poly(ethylene glycol diacrylate) (PEGDA) and/or poly(ethylene glycol acrylate) (PEGA) and poly(ethylene glycol methyl ether acrylate) (PEGMEA) networks, which exhibit high water permeability, excellent rejection of organic components, and good fouling resistance.

We have tested the filtration properties of commercially available membranes with and without fouling-resistant coatings to assess the benefit of these coatings. The coating procedure was optimized to achieve the coated membranes having various coating thicknesses. Scanning electron microscopy (SEM), x-ray photoelectron spectroscopy (XPS), and contact angle measurements have been used to examine surface characteristics of uncoated and coated membranes. Such membranes with crosslinked PEGDA coatings are stable during filtration tests. By choosing an appropriate support membrane (e.g., an asymmetric structure, having a thin top layer with small pore size), pore penetration can be reduced. The filtration results showed that crosslinked PEGDA coatings rendered the membrane surface more hydrophilic, improved its fouling resistance, and increased its solute rejection characteristics. Oil emulsion crossflow filtration tests showed that the water flux of PSF membranes with coatings was four to five times higher than that of uncoated PSF membranes, which led to better overall separation performance of the membrane.

# 2. Background and Introduction

Produced water is the largest single waste stream in oil and gas production (Produced water discharge to the North Sea, 1998). In 2002, more than 14 billion barrels of produced water were handled in the United States alone (Rawn-Schatzinger, 2003; 2004). This water often contains salts, heavy metals, emulsified oil, and other organics (Produced water discharge to the North Sea, 1998; Rawn-Schatzinger, 2003), rendering it unsuitable for human or animal consumption, or even agricultural use. Often, the most viable disposal option is subsurface injection. Subsurface injection costs vary from $0.50 to $1.75 per barrel (Rawn-Schatzinger, 2004), representing annual operating costs of over 7 billion dollars per year for United States oil and gas operators.

However, water is an extremely valuable commodity. In the arid Western and Midwestern States (e.g., Colorado, Montana, New Mexico, Utah, Texas, and Wyoming), produced water could provide a valuable source of irrigation, industrial, and even potable water if the organic content and salinity could be reduced to acceptable limits (Rawn-Schatzinger, 2004). In west Texas, drought-like conditions have resulted in severe water shortages and a steady lowering of the water table (Williams, 2002). In such locations, it would be highly desirable to purify produced water for drinking or other beneficial alternative uses such as wildlife and livestock water impoundments, recreation, fisheries, wetlands, and other agricultural and industrial uses (Rawn-Schatzinger, 2003).

Produced water, therefore, represents an immense opportunity as a new water source for a wide variety of uses. The Environmental Protection Agency (EPA) maintains strict guidelines for water standards through the Clean Water Act (CWA) (Hammer, 2004; Leeden, 1990). The CWA lists legal limits for contaminants, which must be monitored in public water supplies (Hammer, 2004; Leeden, 1990). Acceptable limits are also prescribed for underground injection control, surface discharge, irrigation, and industrial use (Hammer, 2004; Leeden, 1990). These contaminant limits regulate the amount of not only suspended solids and organics but also dissolved organics and contaminants such as metals. The use of produced water for these applications, therefore, requires removing suspended materials such as solids and emulsified oil. Depending on the application and the quality of the produced water, substantial removal of total dissolved solids (e.g., inorganic ions or dissolved organics) may also be required.

A palette of treatment technologies is available for removing organics and/or desalinating produced water. These technologies include reverse osmosis (RO) and nanofiltration (NF) membranes, freeze/thaw evaporation, ultraviolet radiation, chemical treatment with chlorine and other biocides, ion exchange membranes, electrodialysis, distillation, and capacitive desalination. Among these technologies, polymeric RO or NF membranes could represent the most flexible and viable long-term strategy. In water containing up to 45,000 milligrams per

liter (mg/L) of total dissolved solids (TDS), primarily in the form of salt ions, RO membranes are used commercially to remove contaminants to levels that meet or exceed requirements for the applications mentioned above, including human consumption (Peterson, 1993; Scott, 2003). Moreover, polymer membranes are rapidly becoming the technology of choice for water desalination because they are cost effective, small, and simple to operate and maintain (Peterson, 1993). RO membranes have been optimized over the past 3 decades for high water flux and high salt rejection. Current commercial RO membranes can reject 99.5 percent or more of even small ions such as $Na^+$, and a single commercial membrane element (8 inches in diameter by 40 inches long) operating at a feed pressure of 800 psig[1] (55 bar) produces 9,000 gallons per day (gal/day) (34 cubic meters per day [$m^3$/day]) of drinking water from seawater (Product information, 2004). This process typically recovers approximately 35 percent of the water from the feed as drinking water and leaves the remaining 65 percent as a concentrated brine (Scott, 2003). However, if the TDS concentration in the feed water is lower, the fraction of the feed water that is purified (i.e., the recovery) can be higher. The brine is suitable for subsurface injection or further treatment using processes such as evaporation or crystallization to further reduce the amount of brine for injection. In this manner, the amount of produced water to be injected is minimized, and beneficial use is derived from the purified water. If less rigorous salt removal is required for other potential uses of produced water (e.g., agricultural or landscape watering), then less selective, higher flux NF membranes provide even higher production rates of purified water and higher recovery, and can be used to treat produced water with TDS levels in excess of 50,000 mg/L. Moreover, if only emulsified oil and suspended solids removal is required, higher flow, porous ultrafiltration (UF) membranes could be used (Scott, 2003).

However, when commercially available UF, RO, and NF membranes are exposed to a mixture of salt, emulsified oil droplets, and other particulate matter, their lifetime decreases catastrophically due to dramatic and largely irreversible permeate flux reduction which causes fouling of the membranes by organic components (Scott, 2003). Fouling is the most significant roadblock to wider adoption of membrane technology for desalination specifically and water purification in general (Riley, 1990). This research has explored a new approach to dramatically improve the fouling resistance of commercial UF membranes by applying a very thin coating of fouling-resistant polymer to the surface of these membranes. The research focused on optimizing the fouling-resistant polymer coating chemistry and its attachment to UF membranes. We have leveraged our earlier success in this area, where we were able to prepare fouling resistant coatings for ceramic membranes being commercialized for oily wastewater (bilgewater) purification aboard U.S. Navy ships.

[1] Pounds per square inch gauge.

# 3. Conclusions and Recommendations

- One requirement of the support membrane is to have small pores on its top surface to reduce pore penetration by the coating. Asymmetric UF membranes with appropriate surface chemistry resulted in a repeatable coating process. Overall, coated polysulfone (PSF) membranes showed better separation performance than coated poly(vinylidene fluoride) (PVDF) membranes.

- High molecular weight polymer additives in the initial polymerization mixture increased its viscosity thereby reducing its penetration into the pores of the support membrane during the coating preparation.

- Copolymer network dense films with various composition of poly(ethylene glycol diacrylate) (PEGDA) crosslinker, poly(ethylene glycol acrylate) (PEGA), and poly(ethylene glycol methyl ether acrylate) (PEGMEA) were synthesized. Water contents in the initial polymerization mixture had a strong influence on water transport properties (e.g., water uptake and flux) of these coating materials. Crosslinked PEGDA dense films, prepared with 80 weight percent (wt.%) water in the initial polymerization mixture, exhibited a water uptake of approximately 350 percent, and a water permeability of approximately 150 liters per micrometer (L μm)/($m^2$ hr atm), which was 30 times higher than the water permeability for the sample prepared using 50 wt.% water in the initial polymerization mixture.

- Coating layer thickness was varied from 6 to 50 micrometers (μm) on PSF UF membrane by choosing different coating rod sizes. Prepared coated membranes are stable during the filtration test. Membranes with crosslinked PEGDA coatings showed good antifouling properties during oil/water emulsion dead-end and crossflow filtration. Reducing the coating layer thickness and increasing the water content in the prepolymerization mixture improved the water flux. Coated PSF membranes exhibited fourto five times higher flux than uncoated PSF membranes during crossflow tests.

- Soybean oil/water emulsions used in filtration experiments were characterized by optical microscopy and a Coulter counter. Oil droplet size mainly ranges from 0.8 to 3 μm. Higher organic concentration, larger oil-to-surfactant ratio, and longer agitation time yields smaller oil droplets and narrower size distribution.

# 4. Procedure/System Description

## 4.1 Task 1. Emulsion Selection, Preparation, and Characterization

### 4.1.1 Preparation of Oil/Water Emulsion

An appropriate amount of soybean/canola oil (Wesson) and surfactant (DC193) were combined in a ratio of 9:1 (oil/soybean, w/w), added to 3 liters of prefiltered, deionized water and blended together in a steel vessel. To ensure formation of a stable emulsion, the mixture of water, surfactant, and oil was emulsified for 3 minutes at the highest rotational speed (~20,000 revolutions per minute [rpm]) of the blender. The emulsions were then stored at room temperature and used within 24 hours. The concentration of organics in the water (i.e., oil plus organic components of the surfactant) was varied from 30 to 1,500 parts per minute (ppm) by adding different amounts of oil/surfactant mixture to the water. The total organic carbon content in the prepared oil/water emulsions was determined by a total organic carbon analyzer (model TOC5050A) from Shimadzu (Japan).

### 4.1.2 Optical Microscopy

Optical microscopy experiments were conducted at a magnification of 2475X to observe the prepared oil emulsion samples. Images were taken from the top to the bottom of the sample. Droplets in the images were measured to determine their diameter.

### 4.1.3 Coulter Counter

The Coulter counter (Multisizer™ 3, Beckman Coulter) used in this study was from the Civil and Environmental Engineering department at the University of Texas at Austin (UT). An oil/water emulsion sample was drawn through an aperture across which a current existed. As the sample passed through the aperture, oil droplets caused an increase in voltage proportional to the droplet volume. In this way, the Coulter counter generated data related to the number of droplets in a sample and the size of those droplets. A 30-µm aperture tube was calibrated to accurately measure droplets with a diameter or equivalent spherical diameter between 0.8 µm and 16 µm. The measurement was conducted at room temperature, and the emulsion was diluted 25 fold with deionized water before testing. The droplet diameter and distribution were calculated from a minimum of three separate tests using the same sample.

### 4.1.4 Experimental Design

Experimental design software by JMP was used to organize a set of experiments to understand the effects of preparation conditions on the properties (i.e., droplet size and size distribution) of the oil/water emulsions used in the fouling studies. The factors chosen were organic concentration, oil:surfactant ratio, and agitation time. Various organic concentrations (150, 300, 1,000, 1,500, and 15,000 ppm), oil:surfactant ratios (9:1, 6:1, and 4:1), and agitation times (30, 90, and 180 seconds) were considered as representative formulation conditions. Seventeen experiments were performed, and the results were analyzed using the JMP software.

## 4.2 Task 2. Selection of Commercial Membrane Supports

### 4.2.1 Support Membranes

Porous PVDF UF membranes from Pall Corporation with nominal pore sizes of 0.1 and 0.02 μm were selected as support materials for coatings. These membranes are commercially available and are chemically modified by the manufacturer to be either hydrophilic or hydrophobic. Asymmetric PVDF membranes kindly provided by Dr. Tony Allegrezza at Millipore were also considered. PSF UF membranes, which are used by GE Osmonics as the substrate for preparing RO membranes, were also considered as membrane candidates for coating using the materials developed in this program. Representative commercial RO membranes were also included in this study.

### 4.2.2 Scanning Electron Microscopy

A LEO 1530 scanning electron microscope from the Texas Materials Institute was used to obtain the SEM images of membranes. The SEM was operated at a low voltage of 1 kilovolt. The top surface and cross section of the membranes were observed. Membranes were dried in a vacuum oven overnight and coated with platinum before being imaged in the SEM.

## 4.3 Task 3. Synthesis of Fouling-Resistant Coating Materials

### 4.3.1 Formation of Coating Materials

The coatings of interest were prepared via copolymerization of acrylate (I) and diacrylate (II) monomers, leading to the formation of a network of controlled crosslink density (figure 1). The formation of the network was achieved via ultraviolet- (UV) initiated free-radical polymerization. The reaction was performed in a Fisher Scientific UV chamber under irradiation of UV light

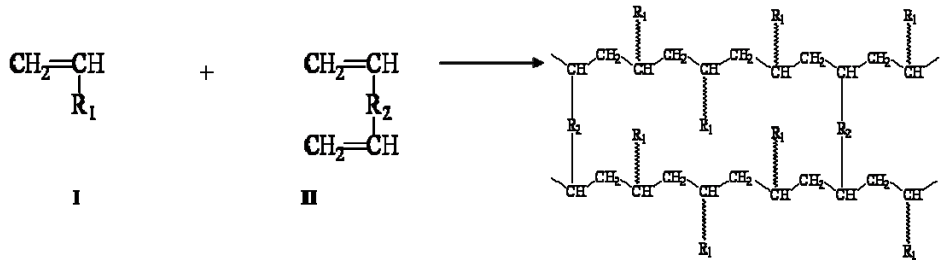

**Figure 1. Structure of the network formed via copolymerization of acrylate monomer and diacrylate crosslinker.**

with a wavelength of 312 nm for 90 seconds to achieve 100 percent conversion of the monomer. 1-hydrooxycyclohexyl phenyl ketone (HPK) was used as the photoinitiator.

## 4.4 Task 4. Preparation of Coated Membranes

### 4.4.1 Preparation of Coated Membranes

The support membranes were soaked in methanol or water to remove any dusts on the top surface and dried in air before coating. Initial polymerization solutions were prepared by mixing PEGDA (*n=13*) crosslinker with water. The water content was varied from 50 to 80 wt.% in the mixture. 2 wt.% high molecular weight poly(ethylene oxide) (PEO) ($M_n$=1,000,000) was added to the polymerization mixture to increase the coating solution viscosity, thereby reducing its penetration into the pores of the support membrane. The prepolymerization mixture was then spread on the top surface of the dried support membranes using a Gardco automatic drawdown machine (figure 2). The coating speed could be adjusted from 1 to 12 inches per second, and the spacer bar distance could be chosen between 6 and 50 μm. The pre polymer coating was polymerized via free-radical polymerization by exposing the coated membrane to UV light for 90 seconds in an argon environment to inhibit oxygen interference with polymerization.

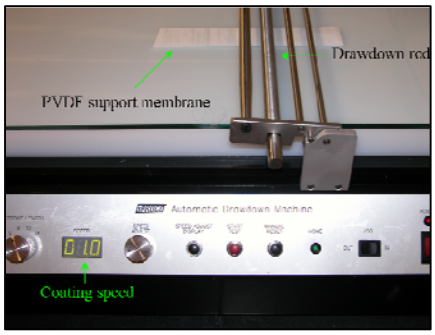


**Figure 2. Automatic coating machine used to prepare coated membranes.**

### 4.4.2 Determination of Coating Thickness

The thickness of the coating layer was estimated using two methods, one based on micrometer readings and the other based on sample weight

(Vankelecom, 1999). In the micrometer method, the thickness of the coated and uncoated support membrane was measured using a micrometer with an accuracy of ±1 μm. The difference between the micrometer readings for the coated and uncoated membranes was recorded as the nominal coating layer thickness by micrometry. In the weight method, the weights of fixed areas of uncoated and coated membrane were measured. The apparent coating thickness was estimated as follows:

$$D = \frac{\left(\frac{W_{coated}}{S_{coated}}\right) - \left(\frac{W_{uncoated}}{S_{uncoated}}\right)}{\rho_{XLPEO}}$$

where $D$ is the apparent coating thickness, $W_{coated}$ is the weight of the coated membrane, $S_{coated}$ is the area of the coated membrane, $W_{uncoated}$ is the weight of the uncoated membrane, and $S_{uncoated}$ is the area of the uncoated membrane;

$\rho_{XLPEO}$, the density of the coating layer, was previously determined to be 1.18 g/cm$^3$.

### 4.4.3 Fourier Transform Infrared/Attenuated Total Reflectance (FT-IR/ATR) Analysis

Attenuated total reflectance-infrared spectroscopy was used to confirm the existence of the coating on PVDF support membranes. The characteristic C=O peak at around 1,725 cm$^{-1}$ was monitored.

### 4.4.4 XPS Analysis

XPS was used to characterize the PSF membranes' surface with and without the coating. Carbon, oxygen, and sulfur were monitored. The mole percent of these elements on the surface was obtained. Theoretically, the C:O:S ratio should be 27:4:1 for PSF membranes and 2:1:0 for a crosslinked PEGDA coating.

### 4.4.5 $CO_2/N_2$ Pure Gas Selectivity

$N_2$ and $CO_2$ gas permeability of coated membranes was measured in a regular gas permeation device. Pure gas selectivity was calculated as the ratio of the permeabilities of these two gases. The selectivity of $CO_2$ over $N_2$ for crosslinked PEGDA (*n=13*) dense films is around 40. These measurements provide a sensitive probe for the presence of defects in the coatings.

## 4.5 Task 5. Characterization of Fouling and Separation Performance

### 4.5.1 Water Uptake

Pure water uptake was measured by the liquid sorption method. The equilibrium amount of liquid water sorbed by a sample film was determined by immersing it in deionized water, blotting it between two pieces of filter paper, and weighing it (Yasuda, 1968). Pure water uptake was calculated using the following equation:

$$S = \frac{W_{swollen} - W_{dry}}{W_{dry}} \times 100 \quad [\text{g-H}_2\text{O}/100 \text{ g-dry polymer}]$$

where $W_{swollen}$ and $W_{dry}$ are the weights of a water-swollen crosslinked polymer film at equilibrium and a dry polymer film, respectively.

### 4.5.2 Dead-end Filtration

Dead-end filtration was conducted at ambient temperature using pure water and an oil/water emulsion as feed solutions. Stirred ultrafiltration cells were purchased from Advantec MFS, Inc, and had a diameter of 43 mm (UHP-43). A flux experiment was performed at constant pressure from 10 to 70 pounds per square inch (psi). The amount of permeate was measured in a graduated cylinder as a function of time. Pure water flux was measured before and after oil/water emulsion filtration. Organic concentration of feed and permeate was determined by total organic carbon (TOC) analysis to estimate rejection.

### 4.5.3 Molecular Weight Cutoff Determination

PEG aqueous solutions were prepared from PEGs having molecular weights ranging from 200 to 35,000. The solution concentration was 0.5 wt. %. These solutions were filtered through membranes in dead-end filtration (Nunes, 1995). Permeate and retentate samples were analyzed by TOC. The molecular weight cutoff (MWCO) is reported as the solute molecular weight at which the rejection is 90 percent.

### 4.5.4 Crossflow Filtration

Crossflow fouling experiments were conducted using a commercial crossflow membrane filtration system (Gueell, 1996). Three membranes can be tested simultaneously at pressures up to 300 psi. All tests were conducted at 25 degrees Celsius ($^{o}$C). Permeate flux was recorded by digital balances connected to a computer. Tests can run for as long as several weeks.

# 5. Research Findings

## 5.1 Task 1. Emulsion Selection, Preparation, and Characterization

Optical microscope photographs of a typical emulsion are shown in figure 3. Several photographs were taken from the top to the bottom of each emulsion sample by varying the focus depth of the microscope. These graphs were scaled based on the standard photographs of mono-dispersed 1-µm and 2-µm latex particles.

(a) (b)

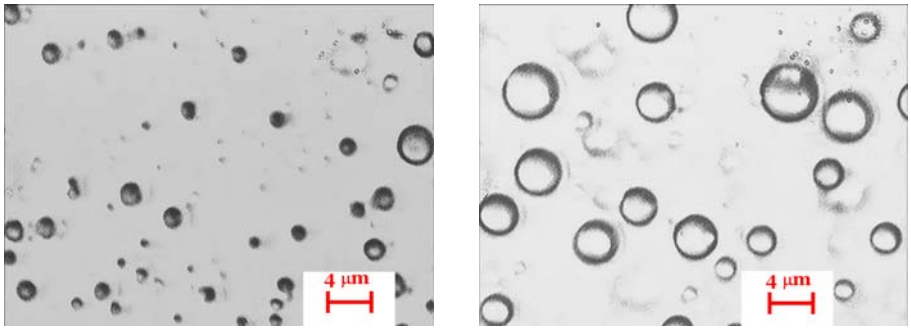


**Figure 3. Optical microscope photographs of oil/water emulsions prepared at (a) 1,500 ppm (organic concentration), 9:1 (oil:surfactant ratio) and 180 seconds (agitation time), and (b) 15,000 ppm, 9:1, and 180 seconds.**

Droplets shown on the graphs were counted and measured. The mean size of the droplets was defined as:

$$D_n = \frac{\sum_i N_i \cdot d_i}{\sum_i N_i} \text{ and } D_v = \frac{\sum_i N_i \cdot d_i^4}{\sum_i N_i \cdot d_i^3}$$

where $N_i$ is the number of droplets with a diameter of $d_i$. The polydispersity of the emulsions was defined as the ratio of the volume average diameter to the number average diameter.

The changes in $D_n$, $D_v$, and polydispersity with organic concentration, oil:surfactant ratio, and agitation time are presented in figures 4 and 5, respectively. The results indicate that all these factors affect the emulsion droplet size in a certain range. Lower organic concentration, more surfactant (i.e., lower oil:surfactant ratio), and longer agitation time yield smaller

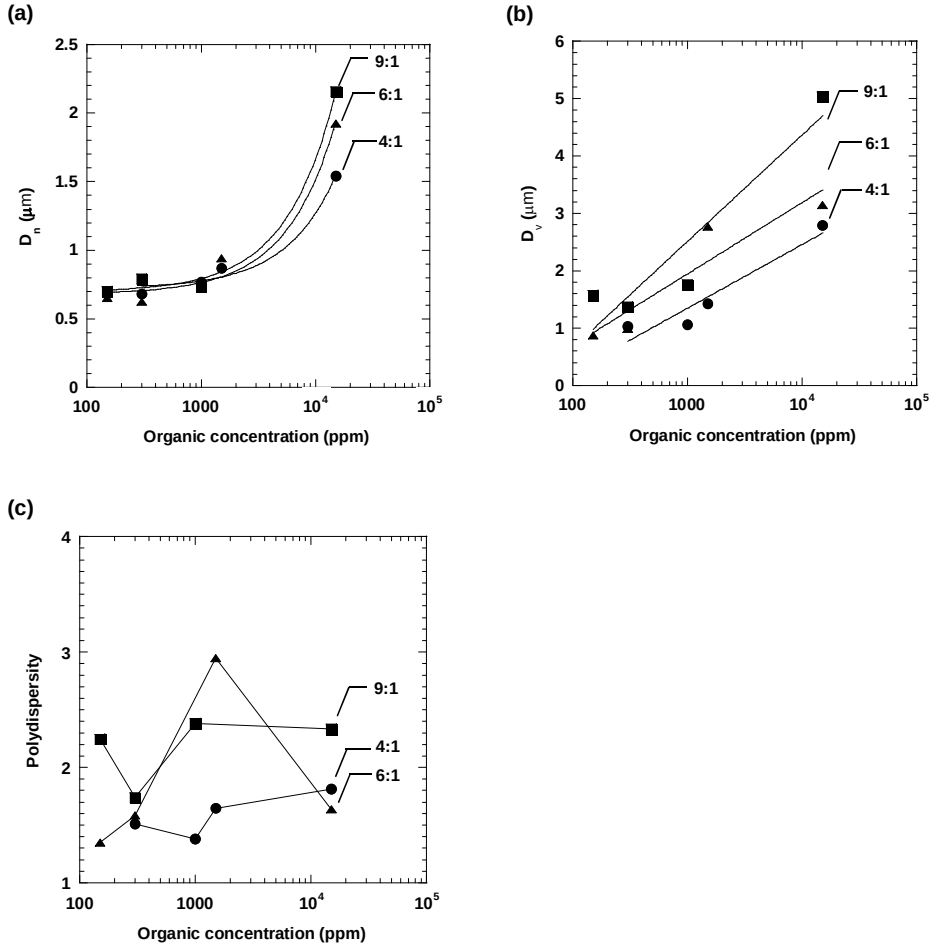


**Figure 4. Relationship between (a) $D_n$, (b) $D_v$, and (c) polydispersity and organic concentration at different oil:surfactant ratios. Optical microscopy was used to characterize the size and size distribution. The agitation time was fixed at 180 seconds.**

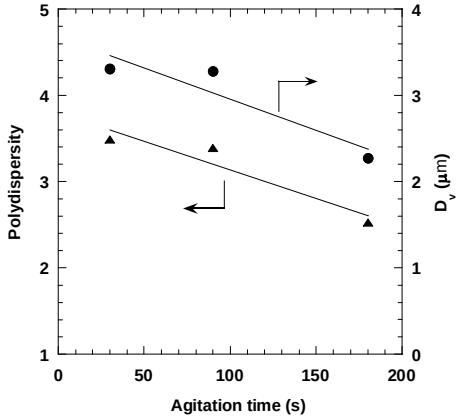


**Figure 5. Effect of agitation time on $D_v$ and polydispersity as measured by optical microscopy. The organic concentration (1,500 ppm) and oil:surfactant ratio (9:1) were fixed.**

droplets. The relationship of polydispersity to organic concentration and oil:surfactant ratio is not clear based on the optical microscopy results.

Typical number average, surface area average and volume average droplet size distributions measured using Coulter counter are presented in figure 6. Emulsions prepared with other organic concentrations, oil:surfactant ratios, and agitation times exhibit similar trends.

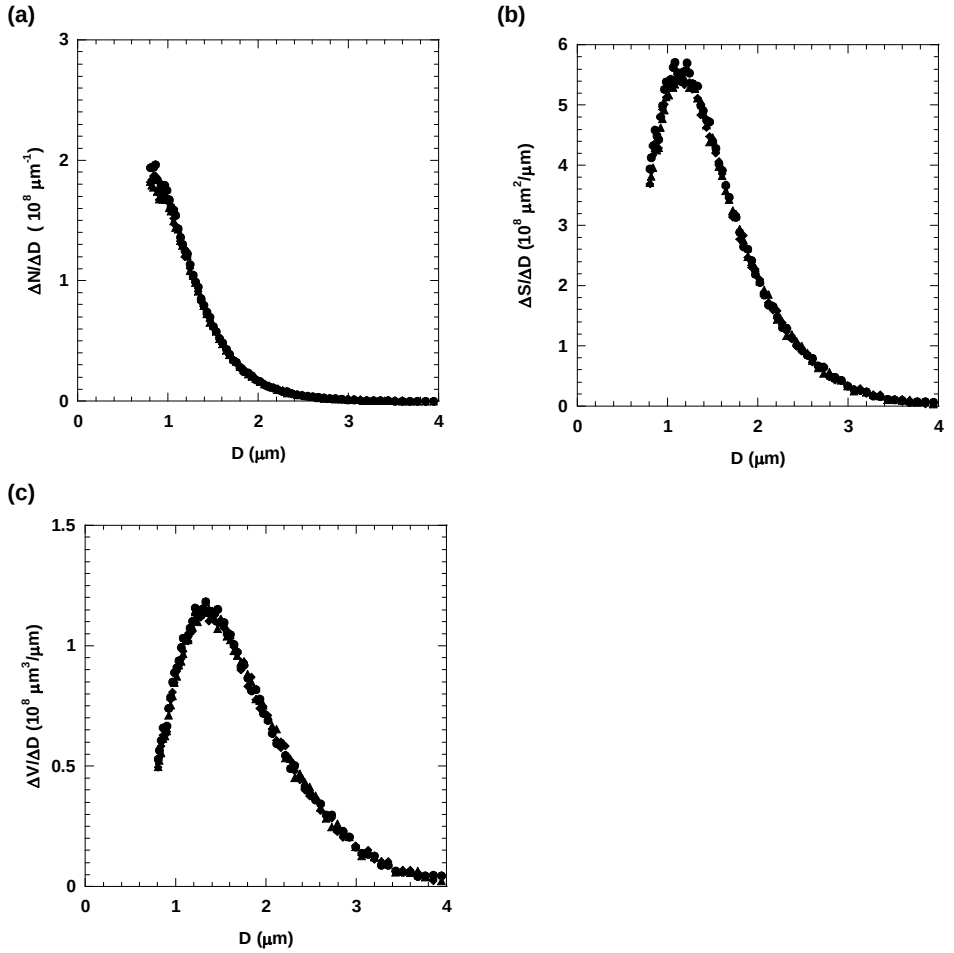


**Figure 6. (a) number average, (b) surface area average, and (c) volume average droplet size distribution of 1,500-ppm soybean oil emulsion (9:1, 180 s) measured using a Coulter counter.**

The stability of the oil emulsions was evaluated by measuring and comparing the droplet size and size distribution of samples prepared using the same conditions as a function of time. In this regard, the droplet size and size distribution were monitored at zero and 24 hours after preparation. The results are presented in figure 7. Little change in the droplet size distribution was observed over the 24-hour time period. $D_n$, $D_v$, and the total number of droplets per unit volume were sensibly equivalent for the zero- and 24-hour aged samples. Based on these results, the emulsions were concluded to be

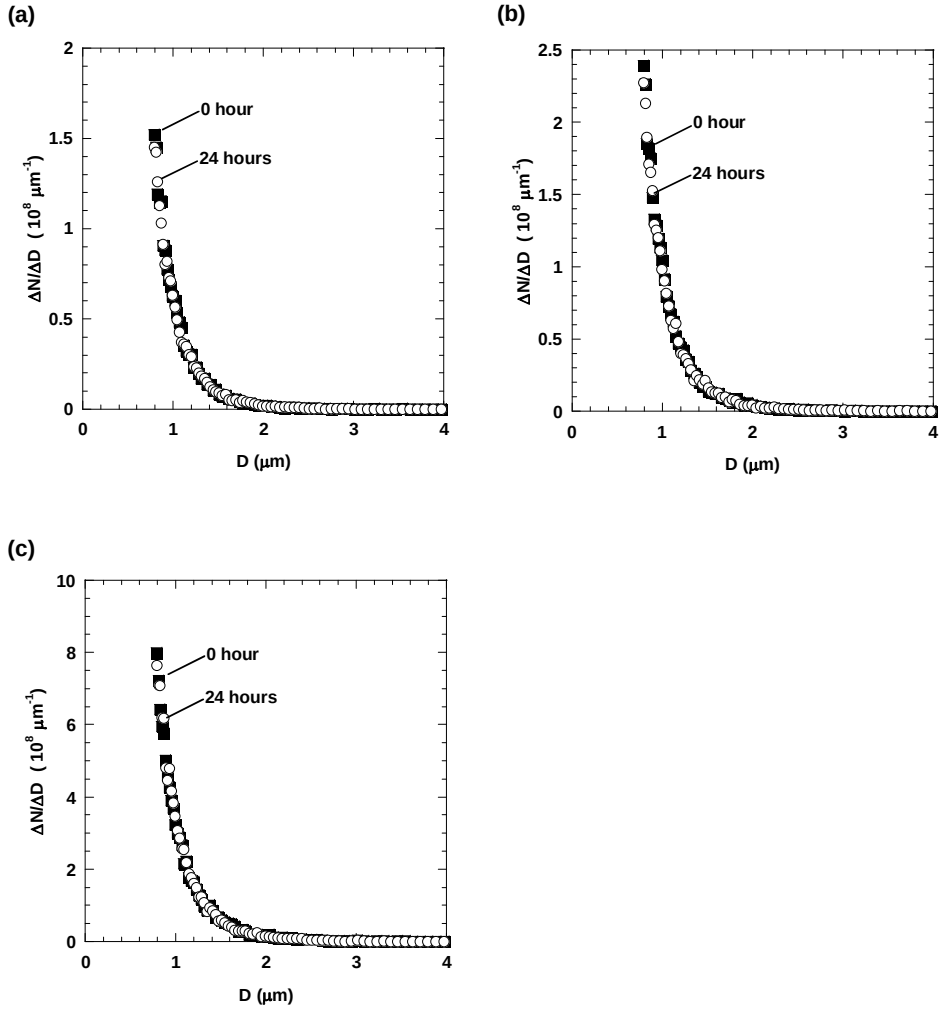


**Figure 7. Droplet size number distribution (a) 150 ppm, (b) 300 ppm, and (c) 1,000 ppm soybean oil emulsion (9:1, 180 s) for 0- and 24-hour aged samples.**

stable for at least 24 hours after preparation. Unless otherwise noted, the membrane characterization experiments were performed within 24 hours of emulsion preparation, so it was important to verify that the emulsions were stable over this time period.

$D_n$, $D_v$, and polydispersity were also calculated for emulsions prepared with varying organic concentration, oil:surfactant ratio, and agitation time based on Coulter counter measurement. The results, shown in figures 8 and 9, were consistent with the optical microscopy measurements and confirmed the previous conclusions. Furthermore, the results showed that well-dispersed emulsions could be obtained at reduced organic concentration or in formulations containing more surfactant than our standard recipe, which is 1,500 ppm oil and surfactant, 9:1 oil:surfactant ratio, and 180 seconds agitation time.

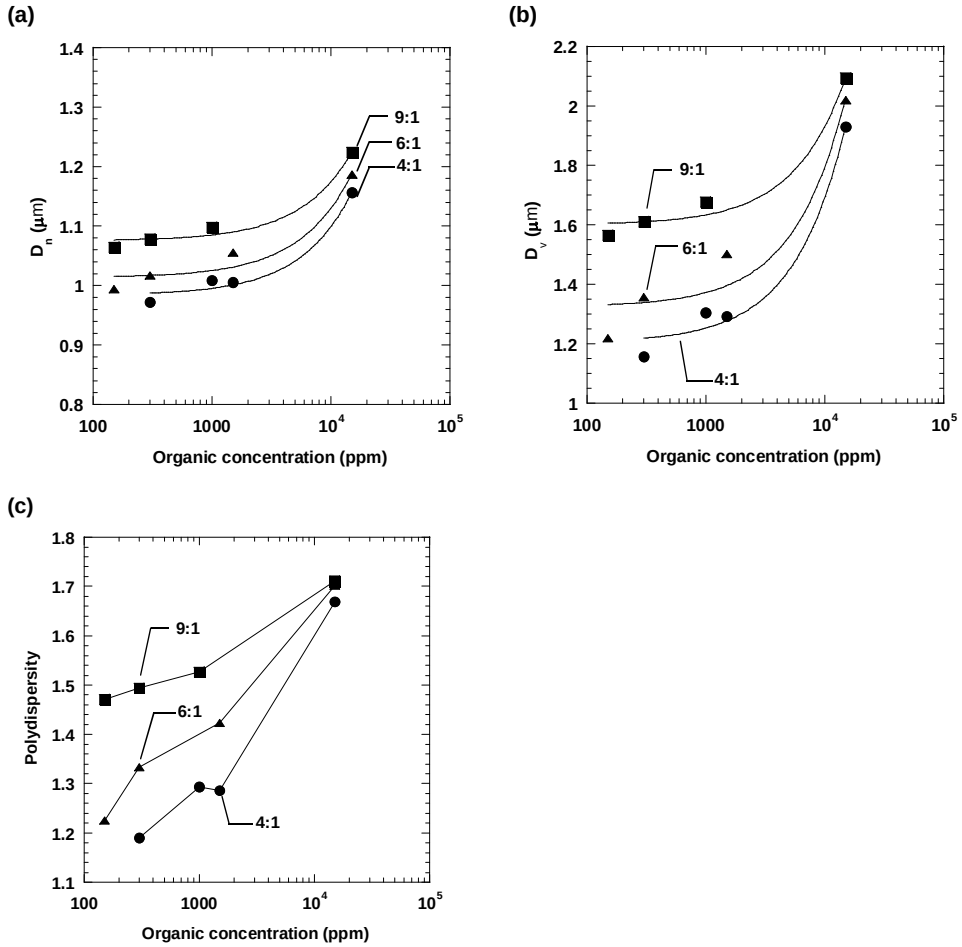


**Figure 8. Relationship between (a) $D_n$, (b) $D_v$, and (c) polydispersity, and organic concentration at different oil:surfactant ratios as measured by the Coulter counter. The agitation time was fixed at 180 seconds.**

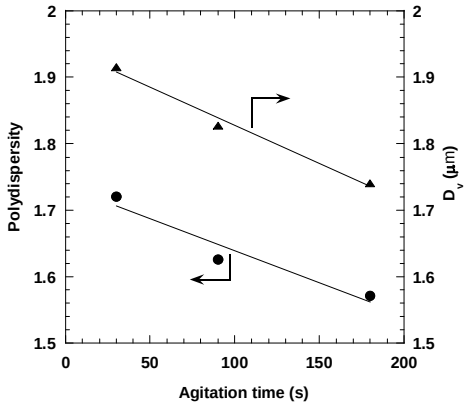


**Figure 9. Effect of agitation time on $D_v$ and polydispersity as measured by the Coulter counter. The organic concentration (1,500 ppm) and oil:surfactant ratio (9:1) were fixed.**

The correlation between number and volume average diameter obtained via optical microscopy and Coulter counter measurements on the same samples is presented in figure 10. The difference in the absolute values reported by each technique was due to different detection ranges of the measurement methods. However, the results given by these two methods were well-correlated.

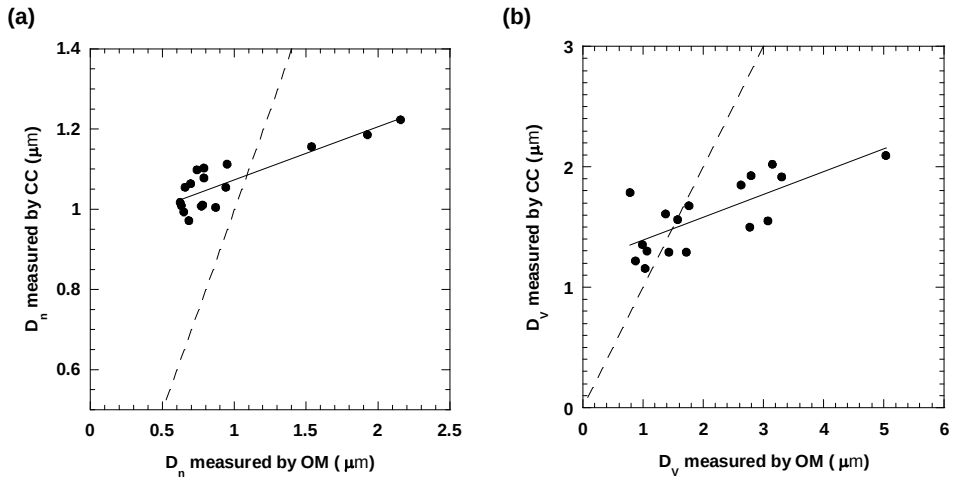


**Figure 10. Correlation of calculated (a) $D_n$ and (b) $D_v$ between optical microscopy (OM) and Coulter counter (CC) measurements. The dashed line is the parity line, which corresponds to the case in which both techniques report exactly the same average diameter for a given sample.**

Emulsions with a variety of average droplet sizes can be prepared using different combinations of organic concentration, oil:surfactant ratio, and agitation time. Organic concentration was the major variable influencing the size and size distribution of the emulsions. Emulsions with smaller droplet sizes and narrower distributions can be achieved by decreasing the organic concentration, adding more surfactant, or increasing the agitation time. The emulsions were stable for at least 24 hours. The impact of droplet sizes on filtration properties will be studied and understood.

## 5.2 Task 2. Selection of Commercial Membrane Supports

Figures 11 and 12 present SEM images of PVDF UF membranes with nominal pore sizes of 0.1 and 0.02 µm. These PVDF membranes all have a lacy surface morphology with a fibrous network structure of interconnected pores. These lacy-structured membranes have a fairly broad pore size distribution, with the pore size on the upper surface of the membrane being larger than the nominal pore size, especially for the 0.1-µm PVDF membranes.

(a) (b)

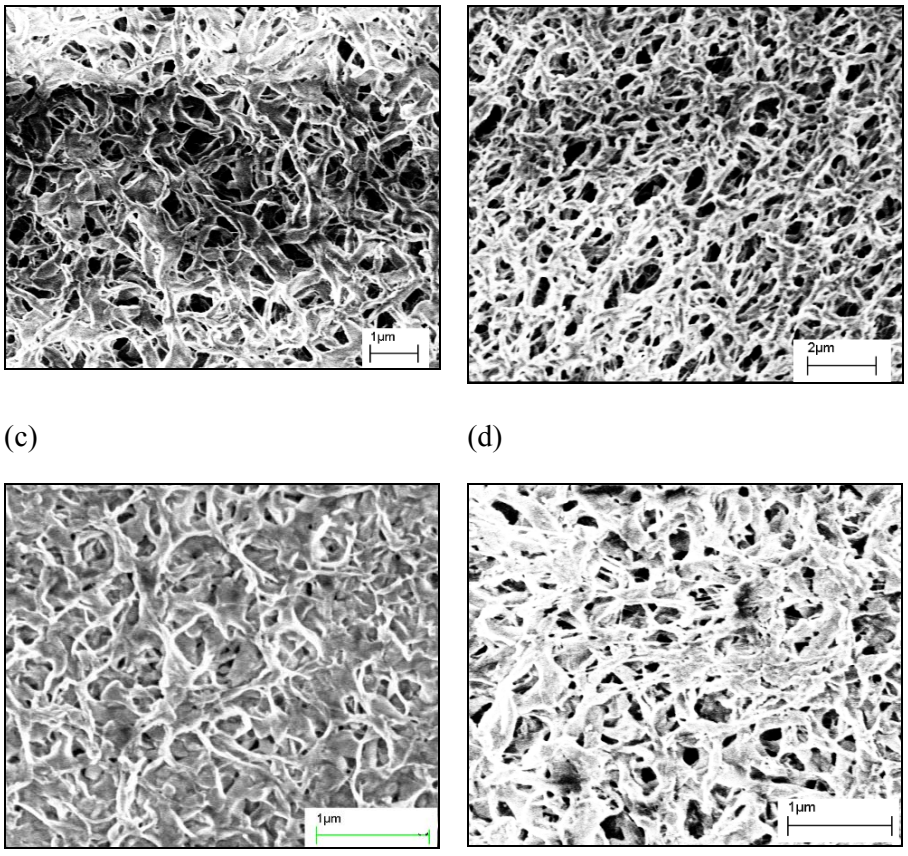


(c) (d)

**Figure 11. Scanning electron micrographs of the surface of uncoated (a) 0.1-µm grafted hydrophilic, (b) 0.1-µm ungrafted hydrophobic, (c) 0.02-µm grafted hydrophilic, and (d) 0.02-µm ungrafted hydrophobic PVDF membranes.**

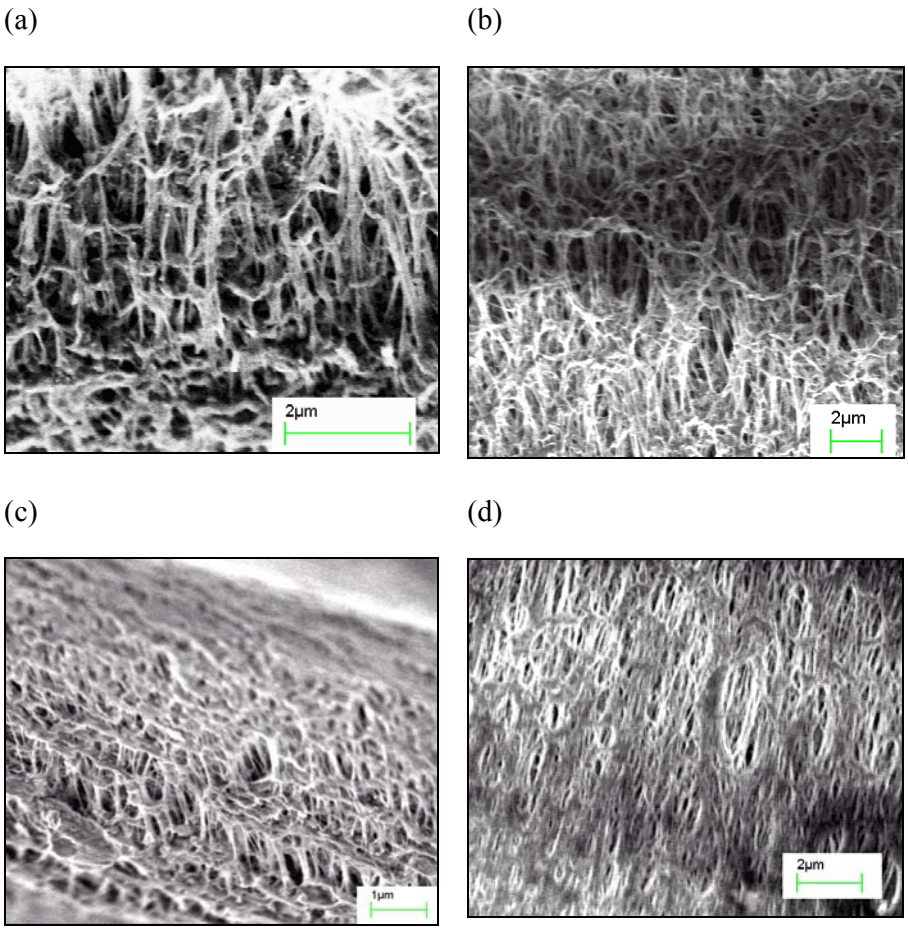


**Figure 12. Scanning electron micrographs of the cross sections of uncoated (a) 0.1-µm grafted hydrophilic, (b) 0.1-µm ungrafted hydrophobic, (c) 0.02-µm grafted hydrophilic, and (d) 0.02-µm ungrafted hydrophobic PVDF membranes.**

Figure 13 presents SEM images of the top and bottom surfaces of asymmetric PVDF membrane provided by Millipore. The top surface had a nodular morphology with small pores and was quite different from the bottom surface.

SEM image of the top surface of a PSF UF membrane is presented in figure 14. The surface had long and narrow cracks, but no apparent pores, at the magnification shown in figure 14. Figure 15 presents SEM image of RO membranes from GE Osmonics. The results prove that these membranes have very small pores at their top surface.

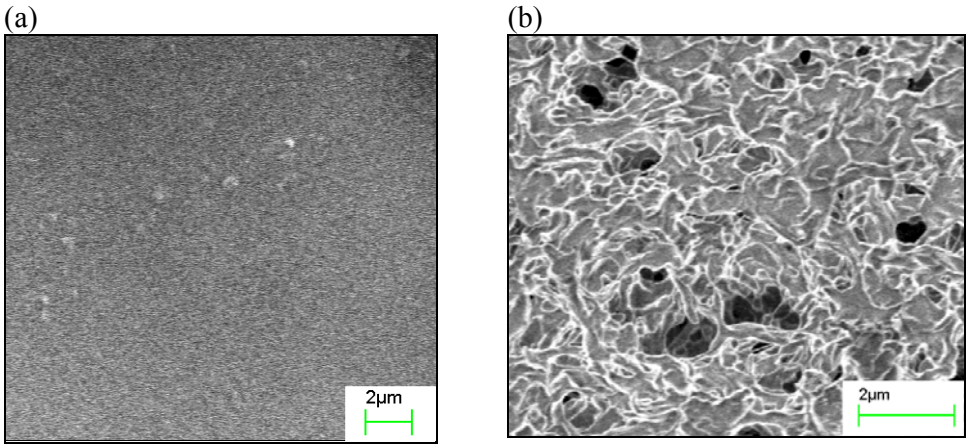


**Figure 13. Scanning electron micrographs of (a) top surface, and (b) bottom surface of the asymmetric PVDF membrane from Millipore.**

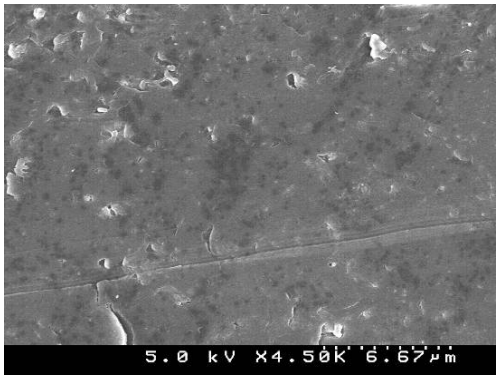


**Figure 14. SEM image of the top surface of a PSF membrane from GE Osmonics. This membrane is the porous support for the aromatic polyamide layer used in the reverse osmosis membrane in figure 15.**

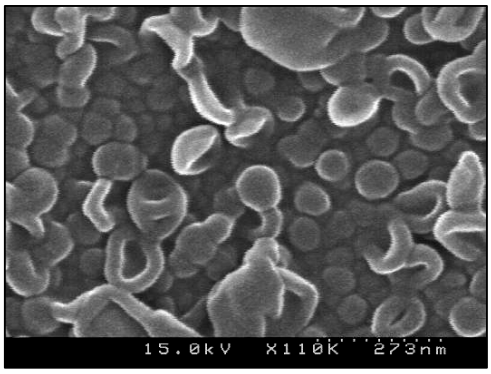


**Figure 15. SEM image of the top surface of a low pressure RO membrane from GE Osmonics (Series AK membrane).**

## 5.3 Task 3. Synthesis of Fouling-Resistant Coating Materials

A series of copolymer networks, prepared by varying the length of the PEGDA crosslinker and the concentration of PEGA and PEGMEA branches, were synthesized, and the effect of these composition variables on crosslink density, water uptake, and transport properties was investigated. During this study, researchers prepared coating materials with the crosslinker, PEGDA (*n=13*). The detailed chemical structure of this starting material is given below:

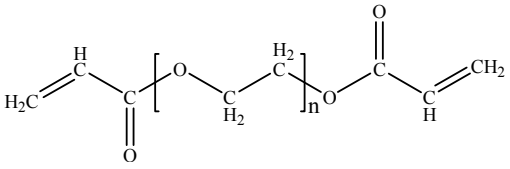

PEGDA

Experiments using different combinations of monomers and crosslinkers were also conducted. The starting materials were commercially available. This family of materials can be used to produce rubbery networks with high water uptake and good water permeability. The structures of the monomers used in the coating formulations discussed below are:

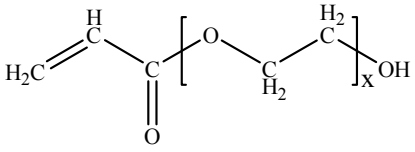

PEGA

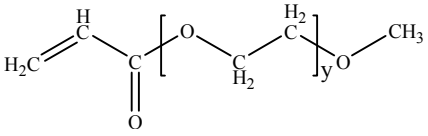

PEGMEA

## 5.4 Task 4. Preparation of Coated Membranes

The effect of photoinitiator concentration in the prepolymerization mixture on coated membrane preparation was first studied. Coated RO membranes were prepared at different photoinitiator concentrations while all other experimental conditions were kept the same. A rod of size 20 was selected for coating, which provides a nominal coating layer thickness of 50.8 μm on an impermeable substrate. The thickness of the resulting crosslinked PEGDA (*n=13*) coating layer was measured by both the micrometer and weight methods. Since the value given by the micrometer method was the thickness of the coating layer on top of the support membrane, and the value given by the weight method was the total thickness of the applied coating material, the difference between these values indicates the degree of penetration of the coating solution into the pores of the porous support membrane. If these two methods give the same result, there is no pore penetration. If the thickness from the micrometer method is less than that by the weight method, there is pore penetration.

The results are presented in figure 16. Four duplicate membranes were prepared for each photoinitiator concentration, and the error bars represented the standard deviation among these samples. A smaller error bar indicated higher reproducibility of the coating process. From these results, using more photoinitiator reduced the oxygen inhibition effect during free radical polymerization and increased the reproducibility of the coating process. Therefore, the photoinitiator concentration was set to 5 wt.% for preparing coating layers without any water in the prepolymerization mixture and was decreased to 1 wt.% when water was present in the prepolymerization mixture to achieve a homogeneous solution because the photoinitiator (HPK) was hydrophobic. Furthermore, the difference between the thickness values given by the two methods (micrometer and weighing) was small, so pore penetration was not a severe problem for the RO support membrane, and was less severe for the asymmetric PVDF and PSF supports than the symmetric PVDF UF membranes.

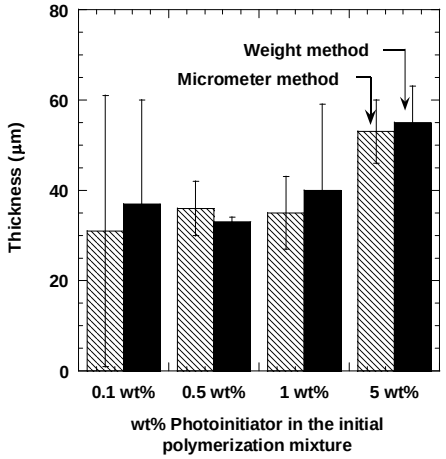


**Figure 16. Thickness of the coating layer on an RO membrane (GE Osmonics Series AK) prepared using crosslinked PEGDA (*n=13*) and different photoinitiator concentrations. In this coating formulation, no water was used in the prepolymerization mixture.**

SEM was also performed to observe the morphology of the coated membranes. Top surface and cross-sectional SEM images were taken for coated membranes prepared with a crosslinked PEGDA coating. The results for a coated 0.02-µm hydrophilic PVDF membrane are presented in figure 17. SEM images for PSF membranes with and without coating are shown in figure 18. Crosslinked PEGDA coating layers were observed on the top and altered the surface morphology of the support membranes. No apparent pores were observed on coated membranes. Additionally, the coating layer thickness is uniform on the PSF membranes.

The FT-IR spectra of the bare PVDF support membrane and the composite membrane are shown in figure 19. The strong absorption at 1,725 $cm^{-1}$ in the spectrum of the coated sample confirms the existence of the PEGDA coating.

(a) (b)

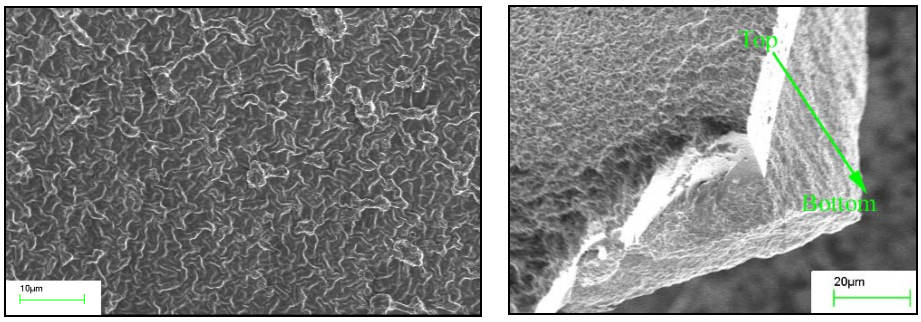


**Figure 17. SEM images of (a) top surface and (b) cross section of coated 0.02-μm grafted hydrophilic PVDF membranes by crosslinked PEGDA (*n=13*) network. In this coating formulation, no water was used in the prepolymerization mixture.**

(a) (b)

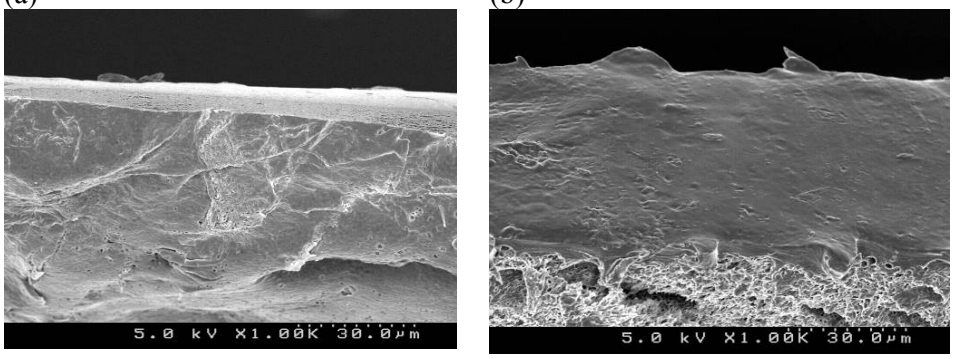


**Figure 18. SEM images of cross section of (a) uncoated and (b) coated PSF membranes by crosslinked PEGDA (*n=13*) network . In this coating formulation, no water was used in the prepolymerization mixture.**

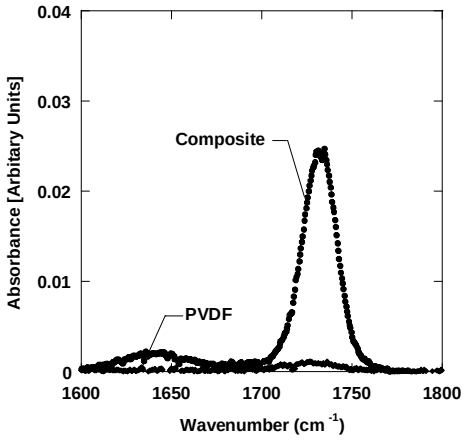


**Figure 19. FT-IR spectra of composite and support PVDF membrane.**

XPS measurement results of bare and coated PSF membranes are presented in table 1. Crosslinked PEGDA coating was prepared without water in the initial mixture. Hence, the molar ratio of carbon to oxygen is approximately 2 to 1. These results prove the existence of the PEGDA coating on top of PSF membranes.

**Table 1. XPS measurements of uncoated and coated PSF membranes**

| Membrane | Carbon (mol. %) | Oxygen (mol. %) | Sulfur (mol. %) |
|---|---|---|---|
| Uncoated PSF | 79.94 | 16.74 | 3.33 |
| Coated PSF[1] | 68.00 | 31.66 | 0.34 |

[1] Coating layer is prepared without water in the initial polymerization mixture.

$CO_2/N_2$ pure gas selectivity tests were performed for crosslinked PEGDA (*n=13*) coated composite PVDF membranes. The selectivity of $CO_2$ over $N_2$ for the composite membranes could reach 19, which was still lower than that of defect-free, nonporous crosslinked PEGDA films (around 40). This result indicates that the coating still has a very low level of defects because the full $CO_2/N_2$ selectivity (40) is not achieved in the coated membrane.

## 5.5 Task 5. Characterization of Fouling and Separation Performance

Water sorption and transport properties of coating materials synthesized with various compositions of PEGDA crosslinker (*n=10, 13*), PEGA monomer, and PEGMEA monomer were investigated via pure water uptake and pure water flux.

Water uptake of the coating materials was tested as a first step to understand their pure water transport abilities. As shown in figure 20, water uptake is greatly dependent on the water concentration of the initial prepolymerization mixture, while it is only slightly affected by the lengths of crosslinker and branch monomers.

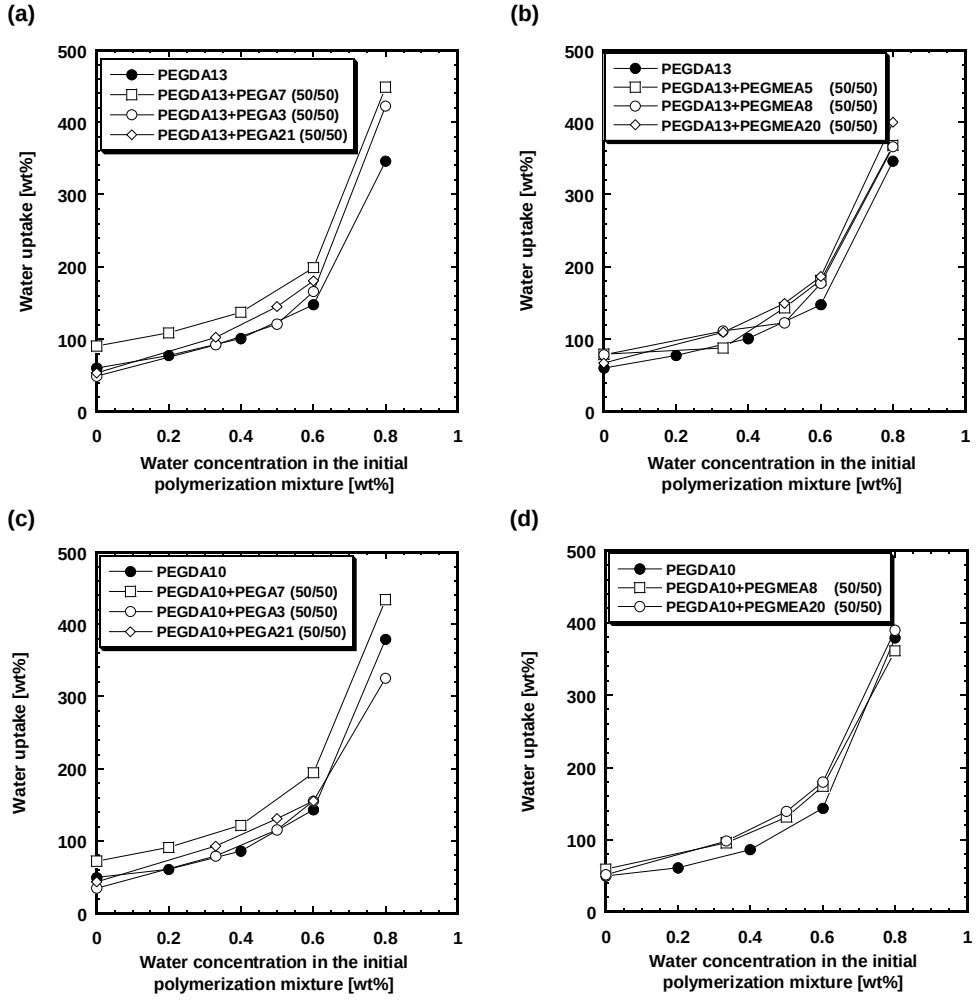


**Figure 20. Water uptake of (a) PEGDA(*n=13*)/PEGA(*n=3,7,21*), (b) PEGDA(*n=13*)/PEGMEA(*n=5,8,20*), (c) PEGDA(*n=10*)/PEGA(*n=3,7,21*), and (d) PEGDA(*n=10*)/PEGMEA(*n=5,8,20*) at different water concentration in the initial polymerization mixture. The numbers in parentheses in the legend indicate the mole percent of each polymerizable component in the coating material.**

The crosslink density of crosslinked coating materials can be estimated based on water uptake results using the Flory-Rehner equation. The results of crosslink density of crosslinked PEGDA (*n=13*) free-standing films are presented in figure 21. Lower crosslink density results in films having higher water uptake. Crosslink density decreases with increasing water content in the initial polymerization mixture.

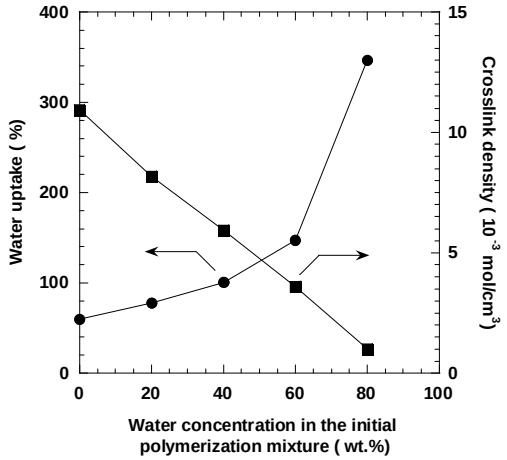


**Figure 21. Water uptake and crosslink density of crosslinked PEGDA *(n=13)* free-standing film with different amounts of water in the initial polymerization mixture. Crosslink density was calculated based on Flory-Rehner expression.**

Figure 22 presents pure water flux of crosslinked dense films with different amounts of water (50-80 wt.%) in the prepolymerization mixture measured at different transmembrane pressure (TMP). Pure water flux is linearly related to TMP over the pressure range explored. Water flux increases greatly as water content increases in the initial polymerization mixture. Free-standing films having 80 wt.% water in the initial polymerization mixture exhibit around 27 times higher flux than the ones prepared with 50 wt.% water.

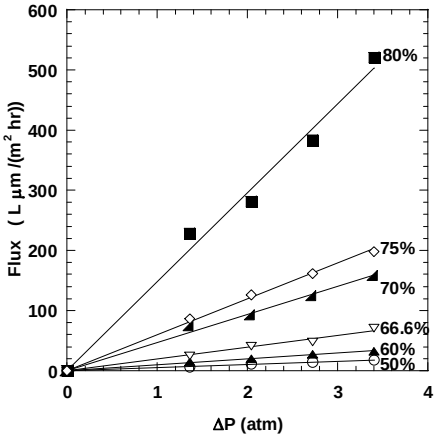


**Figure 22. Water flux of crosslinked PEGDA *(n=13)* free-standing films measured at different TMP. The number in the graph indicates the water contents in the initial polymerization mixture. The thickness of the films is around 300 µm.**

The resistance to flow of free-standing coating materials of known thickness can be characterized from the pure water flux using Darcy's law:

$$J = \frac{\Delta P}{\mu \cdot R_T}$$

where $J$ is the permeate flux, $\Delta P$ is TMP, $\mu$ is the viscosity of the permeate, and $R_{total}$ is the resistance. The resistance of crosslinked PEGDA (*n=13*) free-standing films shown in figure 23 is reported normalized to 1-μm thickness films. Increasing water content in the initial polymerization mixture significantly decreases crosslinked film resistance to water flux.

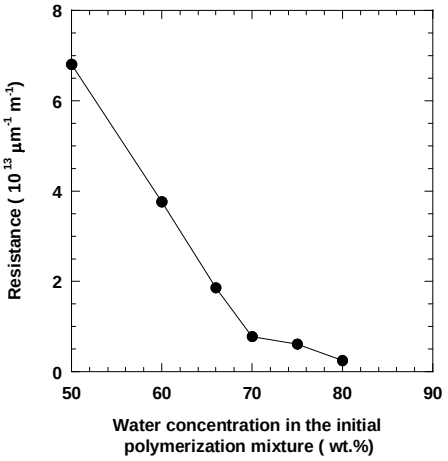


**Figure 23. Mass transfer resistance of crosslinked PEGDA *(n=13)* free-standing films prepared with different water contents in the initial polymerization mixture.**

Pure water flux for various compositions of polymer films that had 60 wt.% water in the prepolymerization mixture are summarized in table 2. The results indicate that adding monomers into the prepolymerization mixture increases the water uptake and water permeability and decreases the crosslink density of the polymer film in a certain range. However, the effects are smaller than the effect of water contents in the initial polymerization mixture. The large pure water permeability increase in polymer films containing long PEGMEA (*n=20*) monomers might result from phase separation induced by polymerization. Those films were opaque instead of clear, and our previous research suggests that such materials can undergo phase separation during polymerization, and this phenomenon increases water flux.

**Table 2. Water transport properties of PEGDA-PEGMEA/PEGA crosslinked polymer films prepared with 60 wt% $H_2O$ in the prepolymerization mixture**

| Network composition (60 wt. % $H_2O$) | | Water uptake (wt.%) | Crosslink density (mol $cm^{-3}$) | Water permeability (L μm/(hr $m^2$ atm)) |
|---|---|---|---|---|
| **Crosslinker** | **Monomer** | | | |
| PEGDA (*n=10*) | None | 143 | 0.0035 | 12.4 ± 1.6 |
| | PEGMEA (*n=8*) | 174 | 0.0028 | 16.8 ± 2.0 |
| | PEGA (*n=7*) | 165 | 0.0031 | 18.7 ± 0.9 |
| | PEGMEA (*n=20*) | 179 | 0.0027 | 69.6 ± 0.9 |
| PEGDA (*n=13*) | None | 147 | 0.0036 | 9.8 ± 1.2 |
| | PEGMEA (*n=5*) | 181 | 0.0027 | 23.4 ± 1.2 |
| | PEGA (*n=7*) | 181 | 0.0027 | 21.3 ± 3.4 |
| | PEGMEA (*n=8*) | 177 | 0.0028 | 18.7 ± 2.2 |
| | PEGMEA (*n=20*) | 187 | 0.0026 | 64.9 ± 8.7 |

*n:* the number of ethylene glycol units in crosslinker PEGDA, monomer PEGA, or monomer PEGMEA, and the ratio of crosslinker to monomer in the prepolymerization mixture is 1:1.

The MWCO characterizes the organic sieving properties of coating materials and membranes evaluated using poly(ethylene glycol) (PEG) of varying molecular weight. Experiment results for crosslinked PEGDA (*n=13*) films, shown in table 3, indicate that adding more water prior to polymerization reduced the sieving properties of coating materials. The result is consistent with a tradeoff relationship between water flux and rejection. Since PEG molecules are much smaller than the oil droplets that were of interest to this study, coating films can still provide high rejection to organic compounds in produced water.

**Table 3. Rejection of PEG molecules by crosslinked PEGDA dense films**

| XLPEGDA dense film | PEG 20000 | PEG 10000 | PEG 3350 |
|---|---|---|---|
| XLPEGDA-66.6%[1] | 98.9% | 99.0% | 98.3% |
| XLPEGDA-75% | 99.3% | 97.6% | 89.6% |
| XLPEGDA-80% | 94.9% | 78.1% | 59.6% |

XLPEGDA: crosslinked PEGDA.
[1] Number indicates the water content in the initial polymerization mixture.

Composite membranes on PVDF supports were prepared from crosslinked PEGDA (*n=13*) that was polymerized with 60 wt.% water in the prepolymerization mixture. Dead-end filtration of pure water and soybean oil/water emulsion filtration experiments were performed on these membranes.

Figures 24 and 25 present the results of uncoated and coated 0.02-μm PVDF membranes. Compared with uncoated PVDF support membranes, the coated membranes showed very good fouling resistance, but low water permeance. The coating layer thickness, shown in table 4, was estimated by the weight and micrometer methods. These coating layers were thick (greater than 150 μm), and the difference between the values given by these two methods was large, indicating significant pore penetration during the membrane coating process. During coating, the initial polymerization mixture apparently wicks into the pores of the membrane; this phenomenon occurs rapidly due to the large pores on the top surface of symmetric UF membranes (such as these PVDF membranes), and this pore penetration by the coating solution reduces water flux significantly. Based on these results, symmetric UF membranes are not preferred candidates for preparing composite membrane for this application.

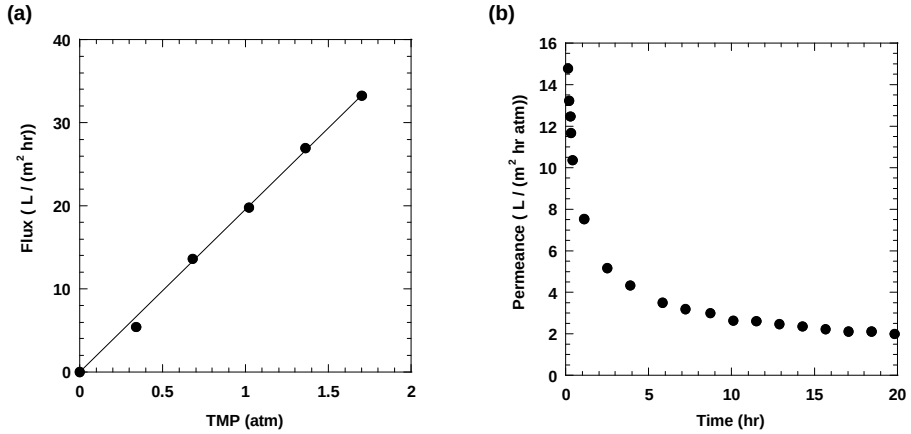


**Figure 24. Dead-end filtration test results of (a) pure water at different TMP and (b) oil/water emulsion (1,500 ppm, 9:1, 180 seconds) for uncoated 0.02-μm hydrophilic PVDF membrane.**

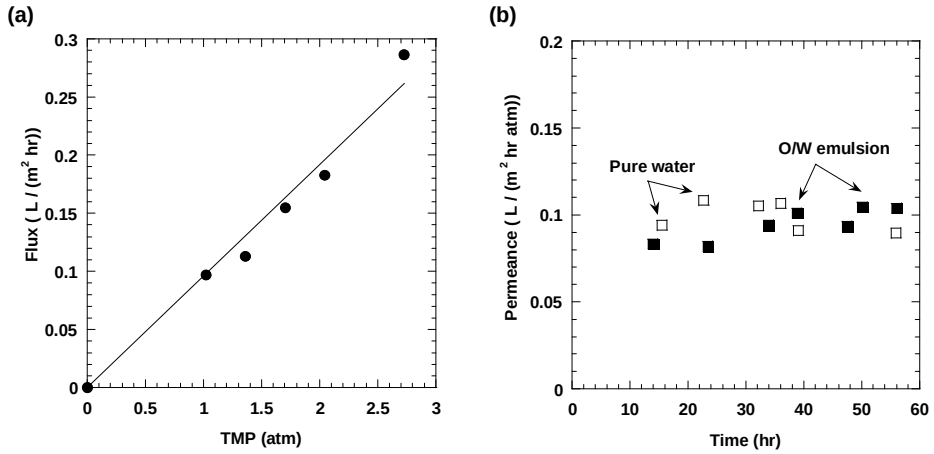


**Figure 25. Dead-end filtration test results of (a) pure water at different TMP and (b) oil/water emulsion (1,500 ppm, 9:1, 180 seconds) for coated 0.02-μm hydrophilic PVDF membrane. In this coating formulation, 60 wt.% water was used in the prepolymerization mixture.**

**Table 4. Coating layer thickness and water flux of coated PVDF membranes**

| Membrane | Micrometer (μm) | Weight (μm) | Measured permeance L/(m$^2$ hr atm) | Calculated permeance L/(m$^2$ hr atm) |
|---|---|---|---|---|
| Coated 0.02-μm hydrophilic PVDF | 153.7 | 165.3 | 0.097 | 0.063 |
| Coated asymmetric PVDF membrane | 159.5 | 149.9 | 0.46 | 0.069 |

Water flux of coated composite membranes can be also related to TMP by Darcy's Law. The total resistance is contributed by the membrane and coating. If no pore penetration occurs, the overall resistance is given by two additive parts, the membrane resistance ($R_m$) and the coating layer resistance ($R_c$):

$$J = \frac{\Delta P}{\mu \cdot (R_m + R_C)}$$

Any pore penetration makes the actual flux lower than the predicted flux. Therefore, the difference between the measured and calculated fluxes provides another measure of the degree of pore penetration. Higher measured flux values indicate unevenness or defects in the coating layer. A comparison between the measured and calculated fluxes of coated PVDF membranes is presented in table 4. The coated PVDF membranes had rather uneven coatings in most cases, mainly due to the low compatibility between PVDF and crosslinked PEGDA.

Pore penetration and low compatibility between the coating materials and support membranes are two major challenges encountered during preparation of coated PVDF membranes. Selected PVDF UF membranes had larger pore size on the upper surface. The relatively large pores on the membrane surface caused severe pore penetration during preparation of coated membranes, which markedly reduced flux. This problem suggests that other support membranes with smaller surface pore size should be considered, and that direction was pursued for this report.

To ameliorate pore penetration, asymmetric PVDF and PSF support membranes were selected for the preparation of coated membranes. Their small pore sizes at the top surface eliminate or markedly reduce pore penetration, and their anisotropic structure can maintain water flux to a large extent. This was important in reducing the pore penetration problem and facilitated control of the coating process.

Pure water and oil emulsion dead-end filtration tests of coated asymmetric PVDF support membranes were performed, and the results are shown in

figure 26. The coated asymmetric PVDF membrane had almost five times higher flux than the coated 0.02-µm PVDF membrane (see figure 25(b)). This result suggests that surface pore size played an important role in controlling pore penetration and increasing the permeate flux of coated membranes. However, the flux of the coated membrane is still significantly lower than that of the uncoated membrane. The coating layer is thick, and the higher estimated thickness given by the micrometer method indicates unevenness of the coating layer (see table 4).

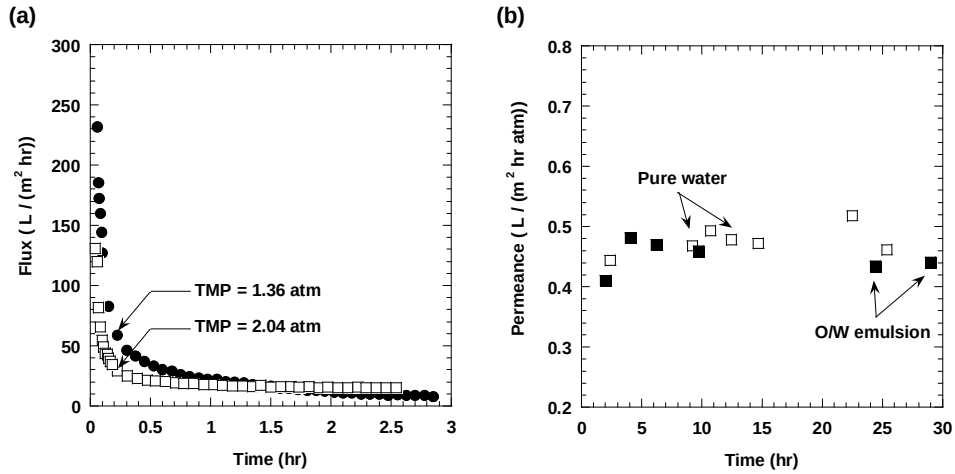


**Figure 26. Oil/water emulsion (1,500 ppm, 9:1, 180 seconds) dead-end filtration test results of (a) uncoated and (b) coated asymmetric PVDF membrane. In this coating formulation, 60 wt.% water was used in the prepolymerization mixture.**

PVDF exhibited low compatibility with crosslinked PEG, mainly due to its hydrophobicity. The initial polymerization mixture did not spread evenly, but rather beaded up on the top surface of the support. Both the support membrane and the coating materials were important for preparing coated membranes. In addition to having similar chemical properties, the support membrane should adhere well to the coating materials. This problem caused the coating process to be less reproducible. Exposing the PVDF support membrane to an alkaline solution prior to coating produces some hydroxyl and carbonyl groups on the polymer chains, which increases the hydrophilicity of the polymer. Filtration studies were conducted on coated alkaline-treated asymmetric PVDF. The results indicated that alkaline treatment maintained the water transport properties of the PVDF membrane and partially improved the reproducibility of the coating process.

Polyethersulfone (PES) and PSF membranes are photosensitive (Yamagishi, 1995). This property should markedly increase the adhesion of the coating materials because the coatings are prepared by polymerizing vinyl monomers on top of underlying membranes via ultraviolet irradiation. This characteristic might be used to help improve the

compatibility of the coating material with the support membrane, perhaps leading to chemical bonding of the PEG coating to the PSF membrane surface.

Coated PSF membranes were prepared with the same procedure, and the process was relatively easy to control and reproducible. Uncoated PSF membranes were first characterized in dead-end oil emulsion filtration test, and the results are presented in figure 27. Results obtained at different TMP showed similar water flux after cake layer formed by the foulant. The resistance increases with decreasing slope, which indicates that external fouling is the dominant mechanism for fouling uncoated PSF membranes (Gueell, 1996).

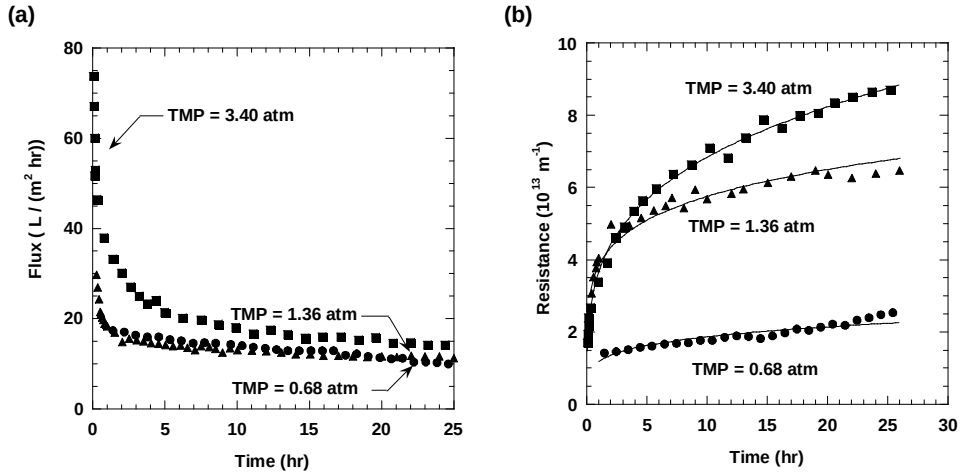


**Figure 27. Oil/water emulsion (1,500 ppm, 9:1, 180 seconds) dead-end filtration tests of uncoated PSF membrane at different TMP. (a) Flux versus Time, and (b) Resistance versus Time.**

Results for coated PSF membranes are shown in figure 28. Coated PSF membranes with a coating layer thickness of 6.9 μm (based on the weight method) had much higher flux than coated PVDF membranes. Similar values of the measured and calculated flux showed that less pore penetration occurred. To further increase water flux, two alternatives were explored: reducing the coating thickness and increasing the water content in the prepolymerization mixture.

The thickness of the coating layer was controlled by choosing the appropriate rod size for the coating machine. Coated PSF membrane samples were prepared using rod size of 10 and 20 (ideally, a size 20 rod yields a coating layer twice as thick as a size 10 rod). Pure water and oil/water emulsion filtration tests were performed on these samples, and the coating layer thickness was measured when the samples were in the hydrated state. The results, presented in figure 29, indicate that water permeance increases

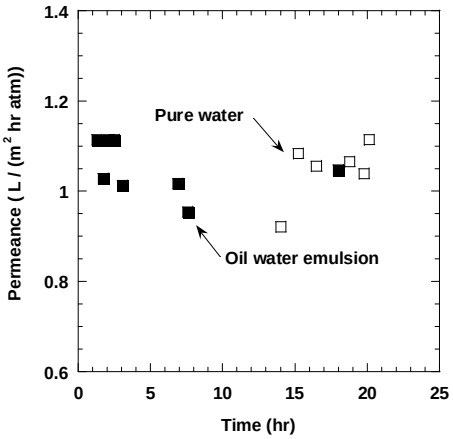


**Figure 28. Oil/water emulsion (1,500 ppm, 9:1, 180 seconds) dead-end filtration tests of coated PSF membranes. In this coating formulation, 60 wt.% water was used in the initial polymerization mixture. Coating layer thickness is 6.9 μm (weight method). The calculated permeance is 1.4 L/(m$^2$ hr atm).**

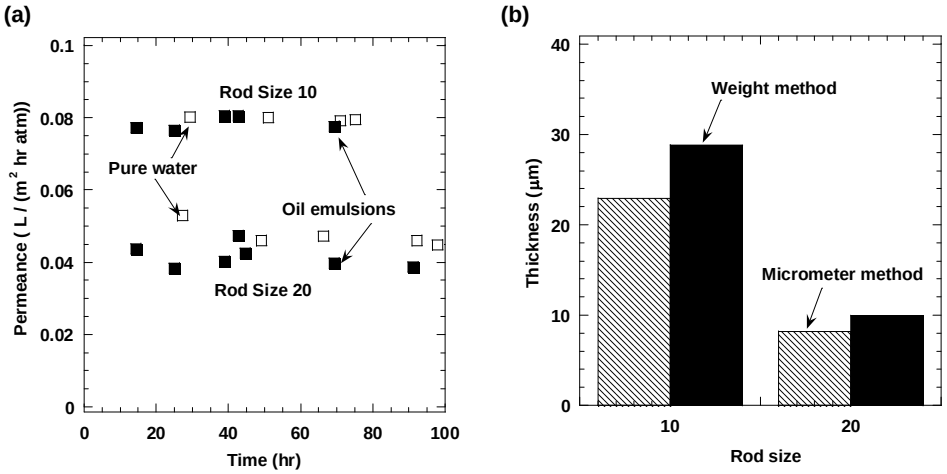


**Figure 29. (a) Permeance of coated PSF membranes with crosslinked PEGDA coating and (b) the thickness of the coating layer. In this coating formulation, 60 wt.% water was used in the prepolymerization mixture.**

significantly when the coating layer thickness is reduced, and there is no change in organic rejection of the coated membrane. Additionally, these coated membranes exhibit essentially no fouling.

Based on previous studies, adding more water to the initial polymerization mixture can significantly affect the water transport properties of the coating layer. The same effect on water flux of coated PSF membranes is presented in figure 30. The results show that increasing water content in the prepolymerization mixture also improves the water flux of coated membranes without reducing their anti-fouling properties. In further composite membrane preparation, 80 wt.% water in the prepolymerization mixture was used.

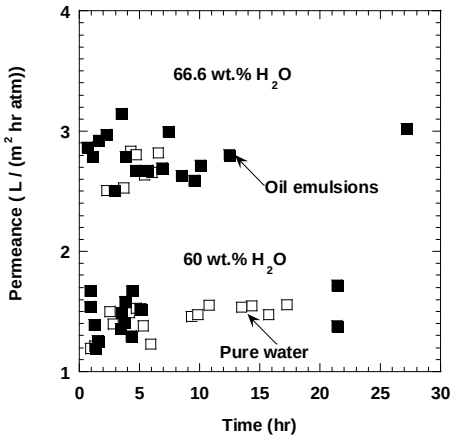


**Figure 30. Effect of water content on water permeance of coated PSF membranes. In this coating formulation, 60 and 66.6 wt.% water was used in the prepolymerization mixture respectively. Rod size 10 was used.**

Captive bubble contact angle measurement was used to determine the relative surface hydrophobicities of coated and uncoated membranes. The contact angle between a soybean oil bubble and the PSF membrane surface with and without coating in water was measured and is reported in table 5. The coated membrane had a much lower contact angle than the uncoated membrane, suggesting that the coating has rendered the polymer membrane surface much more hydrophilic. The enhanced hydrophilicity of the coated membrane should assist in reducing fouling by emulsified oil droplets.

**Table 5. Contact angle of coated and uncoated PSF membranes**

| Membrane | Contact angle (degrees) |
|---|---|
| Uncoated PSF | 131 ± 22 |
| Coated PSF * | 52 ± 13 |

The coating layer is prepared with 80% wt.% water in the prepolymerization mixture.

Oil/water emulsion dead-end filtration tests were performed on coated PSF membranes at different TMP. The results are presented in figure 31. Unlike uncoated PSF membranes, the coated membranes exhibited essentially no fouling. There was a linear relationship between permeate flux and TMP up to 50 psi. The coating layer retarded cake formation on the membrane surface because of its hydrophilic nature, so fouling was reduced.

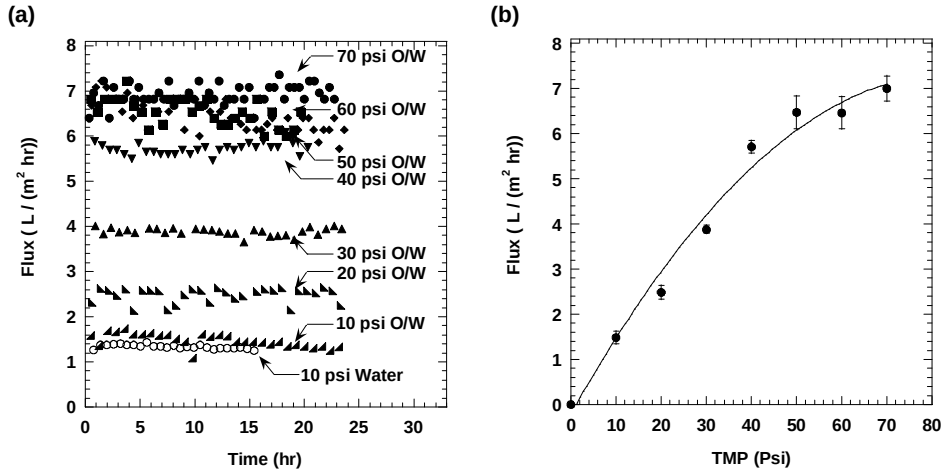


**Figure 31. Water flux versus (a) time and (b) TMP for coated PSF membranes. In this coating formulation, 80 wt.% water was used in the prepolymerization mixture. Rod size 10 was used.**

Further optimization of the coating process for PSF membranes was performed to reduce pore penetration and control coating thickness. Coating layers prepared with small rod size and high water content showed less water transport resistance when compared with previous coated membranes. Oil/water emulsion dead-end filtration was first performed, and the results were presented in figure 32. Rod size 2.5 was used to prepare the coating, and the effective thickness of the coating was 12 μm based on water flux results. Coated PSF membranes showed higher fluxes than uncoated PSF membranes after they got fouled. Duplicate coated PSF membrane samples were prepared and tested. The results illustrated the reproducibility of this coating process.

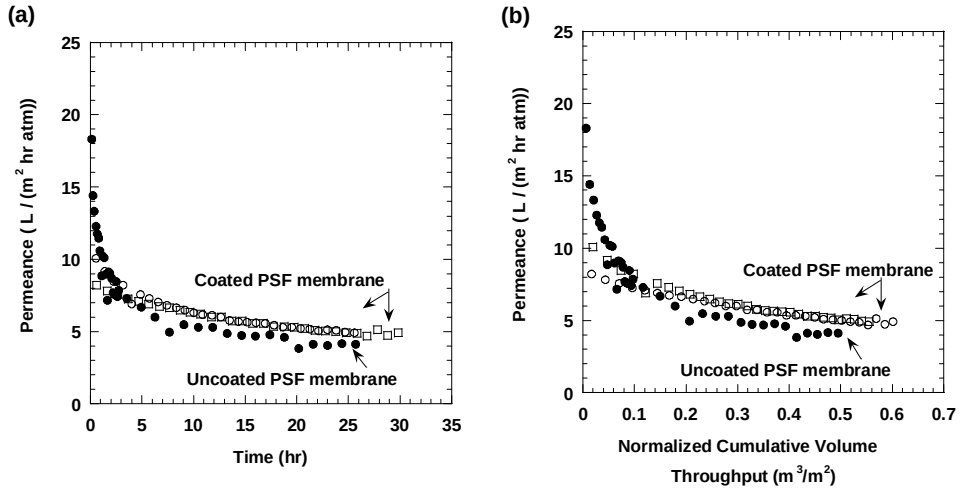


**Figure 32. Dead-end filtration test results of oil/water emulsion (1,500 ppm, 9:1, 180 seconds) for uncoated and coated PSF membrane. In this coating formulation, 80 wt.% water was used in the prepolymerization mixture.**

Since both coated and uncoated PSF showed relatively high rejection to emulsified oil droplets, MWCO experiments were conducted to understand the effect of coating on the membrane particle rejection properties. The results, presented in figure 33, show the crosslinked coating layer provided PSF membrane with higher particle rejection ability.

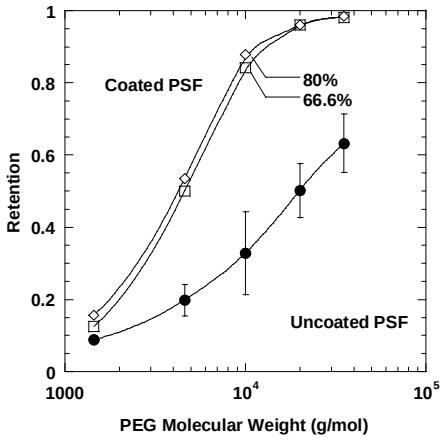


**Figure 33. MWCO results for uncoated and coated PSF membranes. The numbers in the graph indicate the water content in the initial polymerization mixture.**

Crossflow filtration is preferred industrially because the bulk of the feed fluid flow is tangent to the membrane surface in crossflow filtration, so that hydrodynamic forces provide a mechanism to remove external foulants. Oil/water emulsion crossflow filtration tests were performed for uncoated and coated PSF membranes. The experiments were conducted at TMP values of 6.8 and 13.6 atm. Water permeance as a function of operation time was measured, and the results are presented in figure 34. The coated PSF membranes showed almost 5 times higher flux than the corresponding uncoated membranes. The coating also improved fouling resistance of PSF membranes. Experimental results clearly demonstrated the feasibility of the concept of using crosslinked PEGDA coatings to improve the separation performance of membranes.

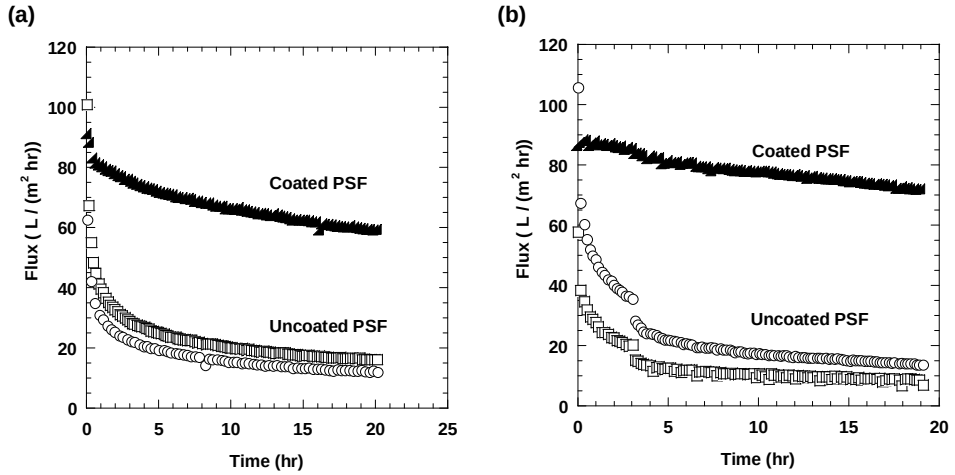


**Figure 34. Oil/water emulsion (1,500 ppm, 9:1, 180 seconds) crossflow filtration tests of uncoated and coated PSF membranes running at (a) 6.8 atm and (b) 13.6 atm. Operation conditions: T=25$^{o}$C, Q=0.3 gpm, and Reynolds numbers=830.**

# 6. References


1998. "Produced water discharges to the North Sea: Fate and Effects in the water column." http://www.olf.no/static/en/rapporter/producedwater/2.html.

2004. "Product Information: FILMTEC SW30-380 Membrane Elements." http://www.dow.com/liquidseps/prod/sw30_380.htm.

Gueell, Carme and Robert H. Davis, 1996. "Membrane fouling during microfiltration of protein mixtures." *Journal of Membrane Science*, 119:2, pp. 269-84.

Hammer, M.J. and Jr. M.J. Hammer, 2004. *Water and Wastewater Technology*: Pearson-Prentice Hall, Upper Saddle River, New Jersey.

Leeden, F. van der, F.L. Troise, and D.K. Todd, 1990. *The Water Encyclopedia, Second Edition*. Chelsea, Michigan: Lewis Publishers.

Nunes, Suzana Pereira, Mauricio Luis Sforca, and Klaus-Viktor Peinemann, 1995. "Dense hydrophilic composite membranes for ultrafiltration." *Journal of Membrane Science*, 106:1-2, pp. 49-56.

Petersen, Robert J., 1993. "Composite reverse osmosis and nanofiltration membranes." *Journal of Membrane Science*, 83:1, pp. 81-150.

Rawn-Schatzinger, V., D. Arthur, and B. Langhus, 2003. "Coalbed Natural Gas Resources: Water Rights and Treatment Technologies." *GasTIPS, 9*, pp. 13-18.

Rawn-Schatzinger, V., D. Arthur, and B. Langhus, 2004. "Coalbed Natural Gas Resources: Beneficial Use Alternatives." *GasTIPS, 10*, pp. 9-14.

Riley, R.L., 1990. "Reverse Osmosis.," in *Membrane Separation Systems - A Research & Development Needs Assessment, Department of Energy*. R.W. Baker, E.L. Cussler, W. Eykamp, W.J. Koros, R L. Riley, and H. Strathmann eds., Springfield, Virginia: Publication number DOE/ER/30133-H1, pp. 5(1)-5(53).

Scott, K., 2003. *Handbook of Industrial Membranes*, Second Edition, Second Printing. Oxford: Elsevier.

Vankelecom, I.F.J., B. Moermans, G. Verschueren, and P.A. Jacobs, 1999. "Intrusion of PDMS top layers in porous supports." *Journal of Membrane Science*, 158:1-2, pp. 289-97.

Williams, D.J., 2002. "West Texas on verge of a water crisis." *USA Today.* http://www.usatoday.com/weather/news/2002/2002-04-07-texas-watercrisis.htm.

Yamagishi, Hideyuki, James V. Crivello, and Georges Belfort, 1995. "Development of a novel photochemical technique for modifying poly(arylsulfone) ultrafiltration membranes." *Journal of Membrane Science*, 105:3, pp. 237-47.

Yasuda, Hirotsugu, C.E. Lamaze, and L.D. Ikenberry, 1968. "Permeability of solutes through hydrated polymer membranes. I. Diffusion of sodium chloride." *Makromolekulare Chemie*, 118, pp. 19-35.

# 7. Data Appendix

**Figures 4 and 5. Oil droplet size of oil/water emulsions measured by optical microscopy.**

| Preparation conditions | $D_n$ (μm) | $D_v$ (μm) | Polydispersity |
|---|---|---|---|
| 150 ppm, 6:1, 180 seconds | 0.65 | 0.88 | 1.35 |
| 150 ppm, 9:1, 180 seconds | 0.70 | 1.57 | 2.24 |
| 300 ppm, 4:1, 180 seconds | 0.68 | 1.03 | 1.51 |
| 300 ppm, 6:1, 180 seconds | 0.63 | 0.99 | 1.57 |
| 300 ppm, 9:1, 180 seconds | 0.79 | 1.37 | 1.73 |
| 1,000 ppm, 4:1, 180 seconds | 0.77 | 1.06 | 1.38 |
| 1,000 ppm, 9:1, 180 seconds | 0.74 | 1.76 | 2.38 |
| 1,500 ppm, 4:1, 180 seconds | 0.87 | 1.43 | 1.64 |
| 1,500 ppm, 6:1, 180 seconds | 0.94 | 2.78 | 2.96 |
| 15,000 ppm, 4:1, 180 seconds | 1.54 | 2.79 | 1.81 |
| 15,000 ppm, 6:1, 180 seconds | 1.92 | 3.15 | 1.64 |
| 15,000 ppm, 9:1, 180 seconds | 2.16 | 5.03 | 2.33 |
| 1,500 ppm, 9:1, 30 seconds | 0.95 | 3.30 | 3.49 |
| 1,500 ppm, 9:1, 90 seconds | 0.97 | 3.28 | 3.39 |
| 1,500 ppm, 9:1, 180 seconds | 0.90 | 2.27 | 2.53 |

**Figure 6. Standard Coulter counter results of oil emulsion (1,500 ppm, 9:1, 180 seconds).**

| Droplet size (μm) | Number distribution ($10^8$ μm$^{-1}$) | Surface area distribution ($10^8$ μm$^2$/μm) | Volume distribution ($10^8$ μm$^3$/μm) |
|---|---|---|---|
| 0.80 | 1.94 | 3.94 | 0.53 |
| 0.82 | 1.94 | 4.13 | 0.57 |
| 0.84 | 1.94 | 4.32 | 0.61 |
| 0.86 | 1.96 | 4.58 | 0.66 |
| 0.88 | 1.84 | 4.49 | 0.66 |
| 0.90 | 1.73 | 4.43 | 0.67 |
| 0.92 | 1.79 | 4.81 | 0.74 |
| 0.95 | 1.78 | 4.99 | 0.79 |
| 0.97 | 1.79 | 5.27 | 0.85 |
| 0.99 | 1.75 | 5.38 | 0.89 |
| 1.01 | 1.67 | 5.38 | 0.91 |
| 1.04 | 1.61 | 5.43 | 0.94 |
| 1.06 | 1.59 | 5.62 | 0.99 |
| 1.09 | 1.54 | 5.71 | 1.03 |
| 1.11 | 1.43 | 5.54 | 1.03 |
| 1.14 | 1.36 | 5.52 | 1.05 |
| 1.16 | 1.30 | 5.54 | 1.07 |
| 1.19 | 1.25 | 5.56 | 1.10 |
| 1.22 | 1.22 | 5.70 | 1.16 |

| | | | |
|---|---|---|---|
| 1.25 | 1.13 | 5.53 | 1.15 |
| 1.28 | 1.05 | 5.35 | 1.14 |
| 1.30 | 0.99 | 5.30 | 1.15 |
| 1.34 | 0.95 | 5.31 | 1.18 |
| 1.37 | 0.85 | 4.99 | 1.14 |
| 1.40 | 0.80 | 4.91 | 1.14 |
| 1.43 | 0.74 | 4.75 | 1.13 |
| 1.46 | 0.70 | 4.72 | 1.15 |
| 1.50 | 0.62 | 4.39 | 1.10 |
| 1.53 | 0.58 | 4.29 | 1.10 |
| 1.57 | 0.52 | 4.02 | 1.05 |
| 1.61 | 0.48 | 3.92 | 1.05 |
| 1.64 | 0.43 | 3.67 | 1.00 |
| 1.68 | 0.39 | 3.47 | 0.97 |
| 1.72 | 0.34 | 3.17 | 0.91 |
| 1.76 | 0.32 | 3.13 | 0.92 |
| 1.80 | 0.28 | 2.88 | 0.87 |
| 1.84 | 0.25 | 2.64 | 0.81 |
| 1.89 | 0.23 | 2.60 | 0.82 |
| 1.93 | 0.21 | 2.42 | 0.78 |
| 1.98 | 0.18 | 2.18 | 0.72 |
| 2.02 | 0.16 | 2.05 | 0.69 |
| 2.07 | 0.14 | 1.84 | 0.64 |
| 2.12 | 0.12 | 1.68 | 0.59 |
| 2.17 | 0.11 | 1.66 | 0.60 |
| 2.22 | 0.10 | 1.48 | 0.54 |
| 2.27 | 0.08 | 1.30 | 0.49 |
| 2.32 | 0.08 | 1.30 | 0.50 |
| 2.38 | 0.06 | 1.14 | 0.45 |
| 2.43 | 0.05 | 1.01 | 0.41 |
| 2.49 | 0.05 | 0.93 | 0.39 |
| 2.55 | 0.04 | 0.84 | 0.36 |
| 2.60 | 0.04 | 0.79 | 0.34 |
| 2.67 | 0.03 | 0.67 | 0.30 |
| 2.73 | 0.03 | 0.65 | 0.30 |
| 2.79 | 0.02 | 0.51 | 0.24 |
| 2.86 | 0.02 | 0.48 | 0.23 |
| 2.92 | 0.02 | 0.42 | 0.21 |
| 2.99 | 0.01 | 0.33 | 0.16 |
| 3.06 | 0.01 | 0.27 | 0.14 |
| 3.13 | 0.01 | 0.26 | 0.13 |
| 3.21 | 0.01 | 0.24 | 0.13 |
| 3.28 | 0.00 | 0.16 | 0.09 |
| 3.36 | 0.00 | 0.16 | 0.09 |
| 3.43 | 0.00 | 0.11 | 0.07 |
| 3.51 | 0.00 | 0.10 | 0.06 |
| 3.60 | 0.00 | 0.10 | 0.06 |
| 3.68 | 0.00 | 0.07 | 0.04 |
| 3.77 | 0.00 | 0.07 | 0.05 |
| 3.85 | 0.00 | 0.07 | 0.05 |
| 3.94 | 0.00 | 0.07 | 0.04 |

**Figure 8 and 9. Oil droplet size of oil/water emulsions measured by Coulter counter.**

| Preparation conditions | $D_n$ (μm) | $D_v$ (μm) | Polydispersity |
|---|---|---|---|
| 150 ppm, 6:1, 180 seconds | 0.99 | 1.22 | 1.23 |
| 150 ppm, 9:1, 180 seconds | 1.06 | 1.56 | 1.47 |
| 300 ppm, 4:1, 180 seconds | 0.97 | 1.16 | 1.20 |
| 300 ppm, 6:1, 180 seconds | 1.02 | 1.36 | 1.33 |
| 300 ppm, 9:1, 180 seconds | 1.08 | 1.61 | 1.49 |
| 1,000 ppm, 4:1, 180 seconds | 1.01 | 1.30 | 1.29 |
| 1,000 ppm, 9:1, 180 seconds | 1.10 | 1.68 | 1.53 |
| 1,500 ppm, 4:1, 180 seconds | 1.01 | 1.29 | 1.28 |
| 1,500 ppm, 6:1, 180 seconds | 1.06 | 1.50 | 1.42 |
| 15,000 ppm, 4:1, 180 seconds | 1.16 | 1.93 | 1.66 |
| 15,000 ppm, 6:1, 180 seconds | 1.19 | 2.02 | 1.70 |
| 15,000 ppm, 9:1, 180 seconds | 1.22 | 2.09 | 1.71 |
| 1,500 ppm, 9:1, 30 seconds | 1.11 | 1.92 | 1.72 |
| 1,500 ppm, 9:1, 90 seconds | 1.12 | 1.83 | 1.63 |
| 1,500 ppm, 9:1, 180 seconds | 1.11 | 1.74 | 1.57 |

**Figure 16. Thickness of the coating layer on RO supports.**

| Photoinitiator conc. wt.% | Micrometer method (μm) | | Weight method (μm) | |
|---|---|---|---|---|
| | Average | Variance | Average | Variance |
| 0.1 | 31 | 30 | 37 | 23 |
| 0.5 | 36 | 6 | 33 | 1 |
| 1 | 35 | 8 | 40 | 19 |
| 5 | 53 | 7 | 55 | 8 |

**Figure 20. Water uptake (g-$H_2O$/100 g-dry polymer) of coating materials.**

| Coating composition | Water content ( wt.%) | | | | |
|---|---|---|---|---|---|
| | 0 | 20 | 40 | 60 | 80 |
| PEGDA (*n=13*) | 59.9 | 77.5 | 100.8 | 147.3 | 346.5 |
| PEGDA (*n=13*) : PEGA (*n=7*) (1:1) | 90.6 | 108.4 | 137.1 | 198.6 | 448.8 |
| PEGDA (*n=10*) | 49.1 | 61.0 | 86.1 | 143.3 | 379.6 |
| PEGDA (*n=10*) : PEGA (*n=7*) (1:1) | 72.6 | 91.6 | 121.4 | 194.7 | 433.9 |

**Figure 21. Crosslink density of crosslinked PEGDA (*n=13*) films.**

| Water contents in the initial polymerization mixture (wt.%) | 0 | 20 | 40 | 60 | 80 |
|---|---|---|---|---|---|
| Crosslink density ($10^{-3}$ mol/$cm^3$) | 10.9 | 8.2 | 5.9 | 3.6 | 1.0 |

**Figure 22. Water flux (L μm/ ($m^2$ hr)) of crosslinked PEGDA (*n=13*) films.**

| Water contents in the initial polymerization mixture (wt.%) | TMP (atm) | | | |
|---|---|---|---|---|
| | **1.36** | **2.04** | **2.72** | **3.40** |
| 50 | 6.4 | 11.5 | 15.0 | 18.0 |
| 60 | 15.0 | 19.8 | 26.7 | 32.0 |
| 66.6 | 25.3 | 40.5 | 48.2 | 70.5 |
| 70 | 74.6 | 92.8 | 125.3 | 158.5 |
| 75 | 87.0 | 126.1 | 161.9 | 198.4 |
| 80 | 228.3 | 281.8 | 383.5 | 520.6 |

**Figure 23. Resistance of crosslinked PEGDA (*n=13*) films.**

| Water contents in the initial polymerization mixture (wt.%) | 50 | 60 | 66.6 | 70 | 75 | 80 |
|---|---|---|---|---|---|---|
| Resistance ($10^{13}$ $\mu m^{-1}$ $m^{-1}$) | 6.80 | 3.76 | 1.87 | 0.78 | 0.61 | 0.25 |

**Dead-end filtration tests results**

**Figure 24.**

**(a)**

| TMP (atm) | 0.34 | 0.68 | 1.02 | 1.36 | 1.70 |
|---|---|---|---|---|---|
| Pure water flux ($L/m^2$ hr) | 5.5 | 13.6 | 19.8 | 26.9 | 33.2 |

**(b)**

| **Time (hr)** | **Permeance ($L/m^2$ hr atm)** | **Time (hr)** | **Permeance ($L/m^2$ hr atm)** | **Time (hr)** | **Permeance ($L/m^2$ hr atm)** |
|---|---|---|---|---|---|
| 0.05 | 15.5 | 2.00 | 5.7 | 9.00 | 2.9 |
| 0.11 | 15.0 | 3.00 | 4.7 | 10.00 | 2.7 |
| 0.20 | 13.5 | 4.00 | 4.1 | 11.00 | 2.7 |
| 0.31 | 12.0 | 5.00 | 4.5 | 12.00 | 2.5 |
| 0.41 | 10.4 | 6.00 | 3.5 | 13.00 | 2.4 |
| 0.50 | 9.7 | 7.00 | 3.2 | 14.00 | 2.3 |
| 1.00 | 7.8 | 8.00 | 3.0 | | |

**Figure 25.**

**(a)**

| TMP (atm) | 1.02 | 1.36 | 1.70 | 2.04 | 2.72 |
|---|---|---|---|---|---|
| Pure water flux ($L/m^2$ hr) | 0.097 | 0.113 | 0.155 | 0.183 | 0.287 |

**(b)**

| **Time (hr)** | **Permeance ($L/m^2$ hr atm) O/W emulsion** | **Time (hr)** | **Permeance ($L/m^2$ hr atm) Pure water** |
|---|---|---|---|
| 13.9 | 0.083 | 15.5 | 0.094 |
| 23.4 | 0.082 | 22.7 | 0.109 |
| 33.9 | 0.094 | 32.2 | 0.105 |
| 38.8 | 0.101 | 36.0 | 0.107 |
| 47.5 | 0.093 | 39.1 | 0.091 |
| 50.1 | 0.105 | 56.0 | 0.090 |
| 56.0 | 0.104 | | |

**Figure 26.**

**(a)**

| Time (hr) | Water flux ($L/m^2$ hr) TMP=1.36 (atm) | Water flux ($L/m^2$ hr) TMP=2.04 (atm) | Time (hr) | Water flux ($L/m^2$ hr) TMP=1.36 (atm) | Water flux ($L/m^2$ hr) TMP=2.04 (atm) |
|---|---|---|---|---|---|
| 0.06 | 210.0 | 120.0 | 0.5 | 34.2 | 21.5 |
| 0.1 | 127.3 | 54.5 | 1 | 21.9 | 18.0 |
| 0.2 | 66.3 | 30.4 | 1.5 | 16.5 | 15.9 |
| 0.3 | 46.6 | 25.0 | 2 | 11.9 | 15.5 |
| 0.4 | 39.4 | 22.5 | 2.5 | 9.1 | 15.2 |

**(b)**

| Time (hr) | Permeance ($L/m^2$ hr atm) O/W emulsion | Time (hr) | Permeance ($L/m^2$ hr atm) Pure water |
|---|---|---|---|
| 2.0 | 0.41 | 2.4 | 0.44 |
| 4.1 | 0.48 | 9.2 | 0.47 |
| 6.2 | 0.47 | 10.8 | 0.49 |
| 9.7 | 0.46 | 12.4 | 0.48 |
| 24.5 | 0.43 | 14.7 | 0.47 |
| 29.0 | 0.44 | 22.5 | 0.52 |
| | | 25.4 | 0.46 |

**Figure 27**

| Time (hr) | Water flux ($L/m^2$ hr) TMP=3.4 atm | Resistance ($10^{13}$ $m^{-1}$) TMP=3.4 atm | Time (hr) | Water flux ($L/m^2$ hr) TMP=3.4 atm | Resistance ($10^{13}$ $m^{-1}$) TMP=3.4 atm |
|---|---|---|---|---|---|
| 0.03 | 77.3 | 1.61 | 5.5 | 21.4 | 5.81 |
| 0.05 | 73.7 | 1.68 | 6.5 | 20.6 | 6.04 |
| 0.1 | 62.9 | 1.97 | 7.5 | 19.7 | 6.28 |
| 0.2 | 51.8 | 2.4 | 8.5 | 19.1 | 6.51 |
| 0.3 | 47.2 | 2.63 | 9.5 | 19.1 | 6.51 |
| 0.4 | 44.4 | 2.8 | 10.5 | 17.4 | 7.15 |
| 0.5 | 42.6 | 2.92 | 11.5 | 16.8 | 7.39 |
| 0.6 | 35.8 | 3.47 | 12.5 | 17.2 | 7.22 |
| 0.7 | 39.4 | 3.15 | 13.5 | 16.5 | 7.51 |
| 0.8 | 38.0 | 3.27 | 14.5 | 15.8 | 7.84 |
| 0.9 | 37.2 | 3.34 | 15.5 | 15.7 | 7.93 |
| 1 | 36.4 | 3.41 | 16.5 | 15.5 | 8.02 |
| 1.1 | 34.2 | 3.63 | 17.5 | 14.6 | 8.53 |
| 1.2 | 35.0 | 3.54 | 18.5 | 14.5 | 8.57 |
| 1.3 | 34.5 | 3.59 | 19.5 | 14.8 | 8.38 |
| 1.4 | 33.2 | 3.74 | 20.5 | 14.7 | 8.46 |
| 1.5 | 31.8 | 3.9 | 21.5 | 14.4 | 8.62 |
| 2.5 | 27.7 | 4.48 | 22.5 | 14.5 | 8.59 |
| 3.5 | 24.5 | 5.07 | 23.5 | 13.9 | 8.93 |
| 4.5 | 23.6 | 5.25 | 24.5 | 14.6 | 8.47 |

**Figure 28**

| Time (hr) | Permeance ($L/m^2$ hr atm) O/W emulsion | Time (hr) | Permeance ($L/m^2$ hr atm) Pure water |
|---|---|---|---|
| 1.3 | 1.11 | 14.0 | 0.92 |
| 1.7 | 1.03 | 15.2 | 1.08 |
| 2.1 | 1.11 | 16.5 | 1.06 |
| 2.5 | 1.11 | 18.8 | 1.07 |
| 3.1 | 1.01 | 19.8 | 1.04 |
| 6.9 | 1.02 | 20.1 | 1.11 |
| 7.6 | 0.95 | | |
| 18.0 | 1.05 | | |

**Figure 29**
**Rod 10**

| Time (hr) | Permeance ($L/m^2$ hr atm) O/W emulsion | Time (hr) | Permeance ($L/m^2$ hr atm) Pure water |
|---|---|---|---|
| 14.4 | 0.077 | 29.3 | 0.080 |
| 25.1 | 0.077 | 51.1 | 0.080 |
| 38.9 | 0.081 | 71.0 | 0.079 |
| 42.8 | 0.081 | 75.2 | 0.080 |
| 69.3 | 0.078 | | |

**Rod 20**

| Time (hr) | Permeance ($L/m^2$ hr atm) O/W emulsion | Time (hr) | Permeance ($L/m^2$ hr atm) Pure water |
|---|---|---|---|
| 14.4 | 0.044 | 27.3 | 0.053 |
| 25.1 | 0.038 | 49.1 | 0.046 |
| 38.9 | 0.040 | 66.4 | 0.047 |
| 42.8 | 0.047 | 92.2 | 0.046 |
| 44.6 | 0.043 | 98.0 | 0.045 |
| 69.3 | 0.040 | | |
| 91.1 | 0.039 | | |

**Figure 30**
**66.6 wt.% $H_2O$**

| Time (hr) | Permeance ($L/m^2$ hr atm) O/W emulsion | Time (hr) | Permeance ($L/m^2$ hr atm) O/W emulsion | Time (hr) | Permeance ($L/m^2$ hr atm) Pure water |
|---|---|---|---|---|---|
| 0.7 | 2.86 | 5.7 | 2.67 | 2.3 | 2.51 |
| 1.1 | 2.78 | 6.9 | 2.69 | 3.7 | 2.52 |
| 1.6 | 2.92 | 7.4 | 3.00 | 4.3 | 2.84 |
| 2.2 | 2.97 | 8.5 | 2.63 | 4.8 | 2.80 |
| 2.9 | 2.51 | 9.5 | 2.59 | 5.4 | 2.64 |
| 3.5 | 3.15 | 10.1 | 2.72 | 6.1 | 2.66 |
| 3.9 | 2.78 | 12.4 | 2.80 | 6.6 | 2.82 |

**60 wt.% $H_2O$**

| Time (hr) | Permeance ($L/m^2$ hr atm) O/W emulsion | Time (hr) | Permeance ($L/m^2$ hr atm) Pure water |
|---|---|---|---|
| 0.9 | 1.67 | 0.9 | 1.19 |
| 1.3 | 1.39 | 1.3 | 1.22 |
| 1.5 | 1.25 | 2.8 | 1.40 |
| 3.4 | 1.36 | 5.3 | 1.38 |
| 3.7 | 1.41 | 6.0 | 1.23 |
| 4.3 | 1.30 | 9.3 | 1.46 |
| 5.1 | 1.52 | 10.8 | 1.55 |

**Figure 31**

| TMP (psi) | 10 | 20 | 30 | 40 | 50 | 60 | 70 |
|---|---|---|---|---|---|---|---|
| Water flux ($L/m^2$ hr) | 1.49 | 2.49 | 3.88 | 5.71 | 6.48 | 6.46 | 7.00 |

**Figure 32**

| Time (hr) | Through output ($m^3/m^2$) | Permeance ($L/m^2$ hr atm) Coated PSF | Time (hr) | Through output ($m^3/m^2$) | Permeance ($L/m^2$ hr atm) Uncoated PSF |
|---|---|---|---|---|---|
| 0.14 | 0.0025 | 8.59 | 0.0333 | 0.0017 | 22.71 |
| 0.25 | 0.0058 | 8.70 | 0.1389 | 0.0086 | 16.46 |
| 0.5 | 0.013 | 8.13 | 0.25 | 0.0143 | 14.34 |
| 0.75 | 0.0201 | 8.36 | 0.5 | 0.0257 | 12.45 |
| 1 | 0.027 | 8.05 | 0.75 | 0.0353 | 11.61 |
| 2 | 0.0538 | 7.70 | 1 | 0.0446 | 10.61 |
| 3 | 0.0795 | 7.38 | 2 | 0.0768 | 9.02 |
| 4 | 0.1043 | 7.21 | 3 | 0.104 | 7.72 |
| 5 | 0.1285 | 6.98 | 4 | 0.1285 | 7.39 |
| 6 | 0.1522 | 6.94 | 5 | 0.1515 | 6.50 |
| 7 | 0.1756 | 6.83 | 6 | 0.1728 | 5.24 |
| 8 | 0.1982 | 6.56 | 7 | 0.193 | 5.91 |
| 9 | 0.2203 | 6.39 | 8 | 0.2124 | 5.95 |
| 10 | 0.2418 | 6.33 | 9 | 0.2313 | 5.26 |
| 15 | 0.3432 | 5.70 | 10 | 0.2496 | 5.21 |
| 20 | 0.4359 | 5.28 | 15 | 0.3343 | 5.24 |
| 25 | 0.5226 | 4.98 | 20 | 0.4117 | 4.24 |
| 30 | 0.6052 | 4.81 | 25 | 0.4843 | 4.22 |

**Figure 33 Retention of PEG molecules**

| PEG molecules g/mol | Uncoated PSF | Coated PSF 60 wt% water | Coated PSF 80 wt% water |
|---|---|---|---|
| 1,450 | 0.09 | 0.13 | 0.16 |
| 4,600 | 0.20 | 0.50 | 0.53 |
| 10,000 | 0.33 | 0.84 | 0.88 |
| 20,000 | 0.50 | 0.96 | 0.96 |
| 35,000 | 0.63 | 0.98 | 0.98 |

**Crossflow filtration results**
**Figure 34**
**(a)**

| Time (hr) | Flux of Coated PSF ($L/m^2$ hr) | Flux of Uncoated PSF ($L/m^2$ hr) | Time (hr) | Flux of Coated PSF ($L/m^2$ hr) | Flux of Uncoated PSF ($L/m^2$ hr) |
|---|---|---|---|---|---|
| 0.028 | 91.2 | 105.6 | 2 | 77.8 | 32.6 |
| 0.033 | 96.0 | 100.8 | 3 | 75.6 | 28.8 |
| 0.083 | 91.2 | 76.8 | 3 | 75.7 | 28.8 |
| 0.133 | 86.4 | 72.0 | 4 | 73.4 | 26.8 |
| 0.183 | 88.3 | 67.2 | 5 | 72.1 | 25.0 |
| 0.233 | 87.0 | 62.4 | 6 | 70.8 | 23.8 |
| 0.283 | 88.3 | 52.8 | 7 | 69.6 | 22.6 |
| 0.333 | 86.0 | 55.0 | 8 | 68.4 | 21.4 |
| 0.394 | 84.0 | 52.0 | 9 | 67.4 | 20.8 |
| 0.444 | 83.4 | 50.2 | 10 | 66.4 | 19.9 |
| 0.494 | 83.2 | 48.4 | 11 | 65.9 | 19.9 |
| 0.544 | 82.6 | 46.6 | 12 | 64.6 | 18.7 |
| 0.594 | 81.7 | 45.7 | 13 | 64.1 | 18.5 |
| 0.644 | 81.3 | 44.8 | 14 | 63.1 | 18.0 |
| 0.694 | 81.4 | 44.0 | 15 | 62.5 | 17.5 |
| 0.744 | 81.2 | 43.0 | 16 | 61.9 | 17.3 |
| 0.855 | 81.0 | 41.3 | 17 | 60.8 | 16.9 |
| 0.905 | 80.9 | 40.5 | 18 | 60.0 | 16.6 |
| 0.955 | 80.9 | 39.9 | 19 | 59.9 | 16.5 |
| 1 | 80.5 | 39.6 | 20 | 59.0 | 16.2 |

**(b)**

| Time (hr) | Flux of Coated PSF ($L/m^2$ hr) | Flux of Uncoated PSF ($L/m^2$ hr) | Time (hr) | Flux of Coated PSF ($L/m^2$ hr) | Flux of Uncoated PSF ($L/m^2$ hr) |
|---|---|---|---|---|---|
| 0.02 | 96.0 | 105.6 | 1 | 87.9 | 48.6 |
| 0.07 | 86.4 | 81.6 | 2 | 86.4 | 40.1 |
| 0.12 | 86.4 | 76.8 | 3 | 85.5 | 35.5 |
| 0.17 | 87.5 | 67.2 | 4 | 82.6 | 23.9 |
| 0.22 | 87.7 | 67.2 | 5 | 81.4 | 22.0 |
| 0.27 | 86.4 | 63.1 | 6 | 78.2 | 20.6 |
| 0.38 | 88.4 | 60.1 | 7 | 79.0 | 19.4 |
| 0.43 | 88.9 | 59.1 | 8 | 78.8 | 18.7 |
| 0.48 | 89.7 | 57.7 | 9 | 78.3 | 18.0 |
| 0.53 | 88.2 | 55.2 | 10 | 78.1 | 17.4 |
| 0.58 | 86.3 | 52.8 | 11 | 77.3 | 16.8 |
| 0.63 | 86.4 | 52.5 | 12 | 76.5 | 16.4 |
| 0.68 | 86.5 | 52.0 | 13 | 75.9 | 15.9 |
| 0.73 | 86.5 | 50.8 | 14 | 75.0 | 15.2 |
| 0.79 | 87.0 | 50.2 | 15 | 74.6 | 15.0 |
| 0.84 | 87.3 | 49.9 | 16 | 74.1 | 14.8 |
| 0.89 | 87.6 | 49.4 | 17 | 73.2 | 14.3 |
| 0.94 | 88.0 | 48.7 | 18 | 72.7 | 14.0 |